Building and Environment 196 (2021) 107796

Contents lists available at ScienceDirect

Building and Environment

journal homepage: http://www.elsevier.com/locate/buildenv

Impact of double skin facade constructional features on heat transfer and fluid dynamic behaviour

Aleksandar Jankovic, Francesco Goia *

Department of Architecture and Technology, Norwegian University of Science and Technology, NTNU, Trondheim, Norway

ARTICLE INFO

Keywords:
Double skin façade (DSF)
Review
Fluid mechanics behavior
Thermophysical behavior
Experimental analysis
Computational fluid dynamics

ABSTRACT

Double skin facades (DSF) are an interesting and important architectural element in buildings as they are visually very attractive and can, at the same time, lead to better performance than single skin facades. DSFs need to be properly designed and operated, or their potential benefits might vanish. For this reason, the physical processes occurring in a DSF should be well understood and predicted. However, they are highly dynamic and in constant interaction with each other, and they depend on the geometric, thermo-physical, optical and aerodynamic characteristics of the different DSF elements. This literature review reports experimental and numerical studies of DSFs that investigate and assess the cause-effect link between constructional features and the thermophysical phenomena occurring in the systems. These studies are analyzed to better understand the current knowledge available to design both naturally and mechanically ventilated DSFs. The review shows that it is possible to understand simple links between families of constructional properties and performance, but only when one parameter at a time is analyzed. General trends can be defined, such as that the optical properties and especially shading (when present) properties are driving factors for both mechanically ventilated and naturally ventilated DSF, while other features seem to be less relevant (at least alone) to determine the behaviour of these systems. However, the complex interaction between more than one constructional feature is seldom investigated, if not completely explored, and this leaves a relatively large knowledge gap to support the optimal design and operation of DSF systems.

1. Introduction

A double skin façade (DSF) is composed of a multi layered structure, most often a highly transparent one, which has an external and internal layer, and a ventilated buffer space in between, sometimes hosting a device for solar and visual gain control [1]. DSFs can assume a different appearance and can be realized with different layouts, usually called Box Window, Shaft-Box, Corridor DSF, and Multi-Storey DSF (Fig. 1), relaying either on naturally induced or on mechanically induced airflow in the ventilated cavity, where by the last one is considered the flow driven by a powered fan.

A double skin façade is, in theory, an advanced system to manage the interaction between outdoors and the internal spaces due to its flexibility [3] thanks to the possibilities enabled by the different airflow paths that can be created in the DSF, ranging from outdoor air curtain to indoor air curtain, from supply air to exhaust air, and to the so-called climate façade configuration, with the possibilities to stop the ventilation flow and obtain a thermal buffer space (Fig. 2).

Besides better thermal performance and abundant daylight, a DSF brings visual attractiveness and provides an improvement in sound insulation, thermal comfort [5]. However, the large glazed surface can underperform conventional envelopes if they are not well designed and managed [6], for example through control of the ventilation flow and the activation of the shading devices in the DSF system [7,8].

The benefits that a DSF brings to the indoor environmental quality are of great interest to the professional and scientific community, while the interaction of DSFs with the outdoor urban environment is a less explored topic. The atypical radiative surface properties of DSF, where the outer skin is often almost fully glazed, may influence the overall energy balance in the urban environment, potentially leading to what is known as the urban heat island effect. However, some latest researches show that, contrary to the negative effect of large vertical glazed surfaces on the urban heat balance, DSF may actually contribute to dampening the urban heat island effect [9–11].

The DSF is widely explored as a technological solution, but it is not straightforward to link the constructional features of a DSF to its thermal

* Corresponding author.
E-mail address: francesco.goia@ntnu.no (F. Goia).

https://doi.org/10.1016/j.buildenv.2021.107796
Received 2 November 2020; Received in revised form 8 March 2021; Accepted 8 March 2021
Available online 16 March 2021

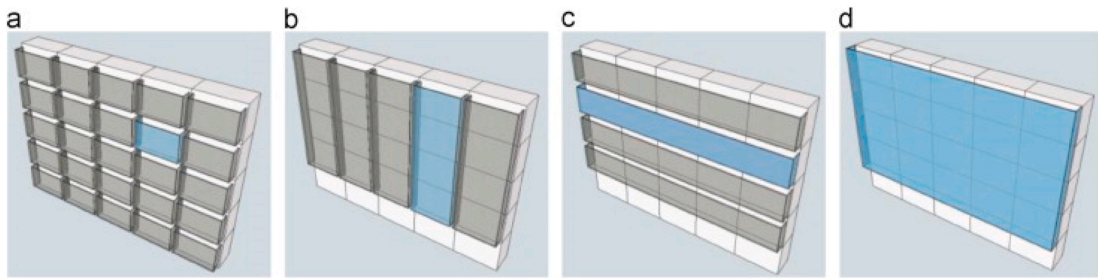

Fig. 1. DSF classification: (a) Box Window, (b) Shaft-Box, (c) Corridor and (d) Multi-Storey double skin façade. Original figure in [2].

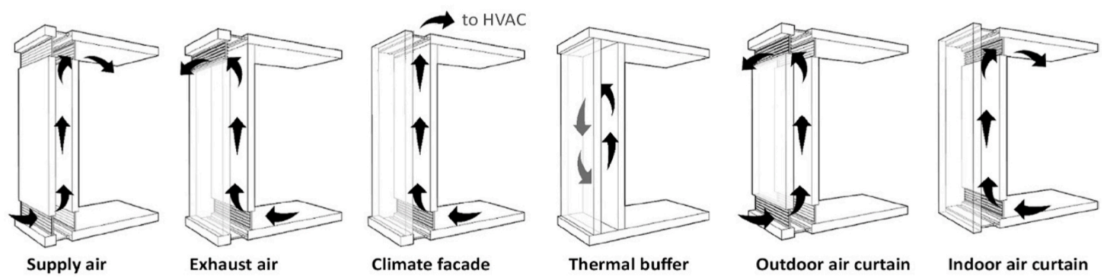

Fig. 2. DSF airflow path alternatives. Derived from illustration in [4].

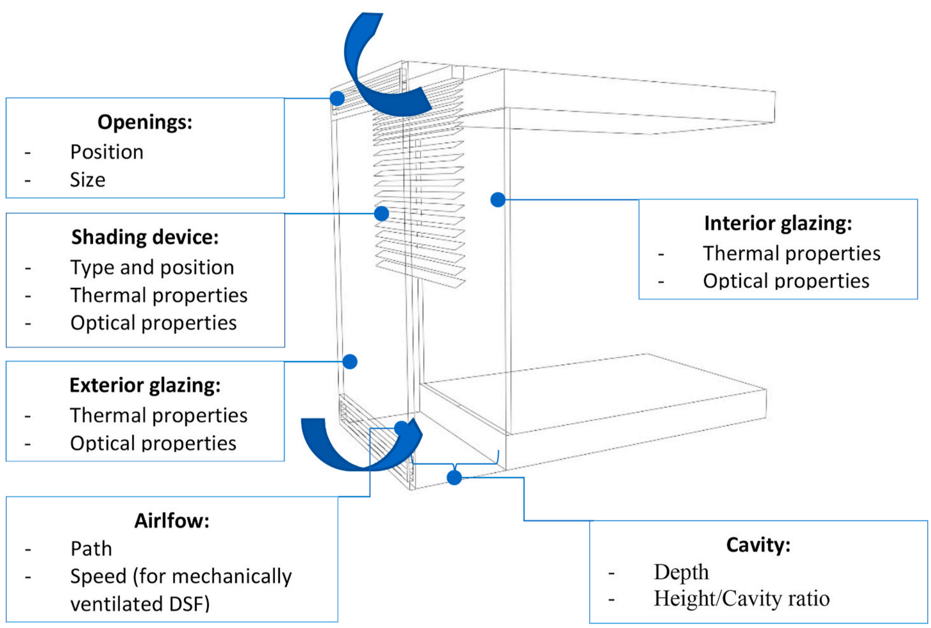

Fig. 3. Schematic representations of the constructional features investigated in this study (exemplified for the case of an outdoor air curtain DSF).

and fluid mechanic behaviour. Transport of mass, momentum, and heat/energy are highly dynamic and in constant interaction, and driven by the indoor and outdoor temperatures, the wind speed and direction, the intensity of incoming/outgoing radiation, and the pressure difference between the cavity and the two surrounding environments. Only once all the physical processes are understood, design actions (e.g. selecting and optimizing the constructional features of the DSF as. geometric, thermo-physical, optical and aerodynamic characteristics) [12] and the operational strategies can be consciously planned to achieve the desired performance goals.

Although much knowledge about transport processes in DSFs is known, we experienced that the literature still lacks a systematic overview of how the constructional configurations of DSFs (e.g. cavity features, shadings, and airflows) affect the performance of a DSF. Through a comprehensive analysis of the established knowledge available in the scientific literature, we aim with this article to: i) explicitly examine the link between constructional features and heat transfer and fluid dynamic behavior in DSF systems; ii) to show how such relationships can be studied; and iii) to identify current knowledge gaps and unexplored relationships. The constructional features that we consider in this work, grouped in Fig. 3 for the different components of the DSF, are:

- geometric features:
  - o dimensions of the cavity;
  - o airflow path;
  - o openings geometry;
  - o shading position (and for venetian blinds, slat angle);
- material properties:

  o glazing properties;
  o radiative surface properties of the shading system;
  o thermal properties of the shading system;
- airflow rate (driven by the fan, only valid for mechanically ventilated DSF).

The main objectives of this article are therefore: to review research articles that clarify the influence how different structural parameters of DSF in conjunction with boundary conditions influence its performance and behavior; through such a review, to highlight what are the best, or at least most used techniques for numerical and experimental analysis of DSF behavior; and finally, to identify the current knowledge, as well as the knowledge gaps and unexplored relationships in the literature.

The identification of the relevant researches for review was done by using the freely accessible web search engines dedicated to scientific literature, using keywords to initiate the search of key documents, and then using a so-called snow-ball method to build up the corpus of manuscripts (articles in journals, and to a lesser extent doctoral dissertations and conference papers) used as a source of information. We also used our own experience and general knowledge of heat transfer and fluid mechanics phenomena to complement and assess the information we found in the literature.

The paper begins with Section 2, with a short part that recalls the theoretical background of heat transfer and focuses on its most complex components, especially for DSF systems, i.e. the convective heat transfer. A systemized overview of experimental and numerical methods to study DSFs is presented in Section 3. Because of the nature of the most complex phenomena occurring in the DSF, after a brief general classification, when talking about numerical methods we place the focus on computational fluid dynamics (CFD) approaches, as they are the most advanced simulation technique to unveil the relationship between constructional features and fluid mechanic behaviour. In Section 4, based on the lessons learned from the literature, we summarize the explicit links between different families and sub-categories of constructional parameters and the fluid mechanics and thermal behavior of DSFs. The article is concluded with Section 5, where we give a comprehensive overview of the identified current know-how and knowledge gaps to be explored in the future to support a more grounded design of DSFs.

2. Theoretical background

The prediction of the thermal performance of a DSF is sensibly more complex than for other building envelope systems. The temperature field in the solid/fluid layers of a DSF is determined by the heat transfer mechanisms occurring in the layer and in the surroundings, which can be a combination of conductive, radiative and convective components. The weight of conduction in the total heat transfer in a DSF is almost negligible, is well understood, and usually modeled within each glass layer or shading if it is present, while it is disregarded in the air channel. Heat transfer by radiation (also called thermal radiation) occurs between glass layers, between these and the shading, and between the interfaces of the DSF and the surrounding environments. Radiative heat exchange, as all the other mechanisms, is strongly influenced by solar radiation absorption and other optical phenomena [13] of the glass panes and the shading surface. The physical-mathematical background behind these two modes of heat transfer is well understood [14] and is not particularly complex in DSFs. Likewise, the numerical modeling of these two types of heat transfer does not pose real problems.

Conversely, the main uncertainty in the prediction of thermal performance of DSF originates from convective heat transfer and more complex knowledge on its physical and numerical background. The convective heat transfer is in its most general form described by the Newton law of cooling, where it is assumed that a rate of heat transfer by convection is proportional to the difference between surface and fluid temperature at an undisturbed location. In engineering practice, for internal flows such as double-skin facades, local temperature difference along cavity should be known, which is dependent on the distribution of both, temperature and velocity inside the cavity and on the surface of the glazing.

For conduits such as the ventilated gap in a DSF, there are several additional factors/influences that brings complexity and stochasticity in a calculation, e.g. asymmetrical boundary conditions and mutual impact of bordering surfaces which is why the entire temperature field across the cavity is affected simultaneously by more than one convective heat exchange. Drivers of the flow vary inconsistently (solar radiation intensity and incident angle, outdoor temperature and especially wind speed and direction), which introduces unsteadiness and randomness in the flow. If geometrically complex elements such as venetian blinds are part of a conduit and if the dependence of thermophysical properties of air and solid parts on temperature is considered, then identification of the relevant quantities describing heat transfer by convection (heat transfer coefficient, Nusselt number etc.) is much more complicated than for more general cases. Before numerical methods became more widely adopted because of increased possibilities given by available computational power, empirical and dimensional analysis have been usually employed for a development of relationship for Nusselt number and evaluation of heat transfer by convection. Nowadays, computational fluid dynamics (CFD) methods are considered suitable tools to obtain a comprehensive solution to these problems [15].

3. Research methods to investigate the thermal and fluid mechanics phenomena in DSFs

This section gives a brief description of the different modelling approaches and the reason why CFD modelling is the best approach to offer a full insight into the cause-effect relationship between different variables in DSFs. Experimental studies represent the first and more reliable source of information, though they suffer from the lack of flexibility given by CFD studies. Furthermore, experiments are very important as they represent the only way of calibration and validation of numerical models.

3.1. Numerical analysis

A detailed numerical modelling of DSFs that wants to address the full complexity of these systems requires the combined representation of heat, mass, and momentum transfer [16]. Modeling and simulation of fluid dynamics in the DSF cavity requires a high degree of accuracy/detail to achieve a high degree of fidelity representation of the reality, and it is only possible to obtain with a specific type of numerical modelling (CFD or multi-zonal approach). However, different approaches to the modelling of phenomena in DSFs are seen with a different degree of accuracy, depending on the overall goal of the modelling activity. These approaches can be grouped in three categories, ranked in growing order of complexity of the model of the air cavity, according to the following list: 1) simplified models, 2) zonal models and 3) CFD models [17].

Simplified models are the broadest category of models that is the least detailed and accurate. Simplified models cover different subcategories, such as: analytical and lumped, airflow-network and control volume models and models derived from the non-dimensional analysis [18]. They are able to predict the thermal performance of DSF by means of simulating heat and mass transfer through bulk airflow rates, but they cannot simulate fluid dynamics (momentum transfer). The most frequently used type of simplified model are lumped models, which are usually employed for parametric optimization analysis, representation of the overall thermal characteristics of the DSF systems, and prediction of the energy performance of DSF as a design assisting tool [19]. They usually are mono-dimensional and assume constant temperatures on the surfaces and cavity of the DSF [17], where heat transfer is represented by Newton law of cooling and occurs between more than two isothermal boundaries. The solution is obtained by the construction of a thermal network characterized by a fictitious thermal resistances and capacitances [20]. Furthermore, building energy simulation tools couple the airflow network with thermal network in order to account the influence of airflow and pressure fields on heat transfer [21]. However, these models are represented by approximate relations, which do not reflect the thermal phenomena in detail and are, because of their intrinsic limitation, not fully representative of the complex interacting phenomena.

In order to overcome these issues, an extension of the Newton formulation was proposed by Foroushani [22], where the convective heat transfer is represented by interaction between each pair of isothermal boundaries characterized by multiple functionality coefficients. The values of these multiple functionality coefficients can be calculated analytically or numerically by the so-called *dQdT technique*, which also can determine the limits of the applicability of the resistor-network model to the convection problem [23]. The extended Newton formulation and the *dQdT technique* were applied with a success to a wide variety of problems: natural [24,25] and forced convection [26,27], laminar [24,26] and turbulent flows [25,28], developed [26, 29] and hydrodynamically developing flows, constant- and variable-property flows [22]. This technique can be used for the improvement of accuracy of lumped models and calculation of more accurate convection coefficients (including heat transfer coefficient) for a wide range of DSF configurations, while still keeping the computational requirements for the simulation at a much lower level than for fully explicit models.

Zonal models are more advanced representations than lumped parameter models and other types of simplified models. They offer an intermediate approach with half-way accuracy and computational cost between CFD and control-volume models. Zonal models divide the DSF system into coarse cells (larger than cells in CFD models), where conservation laws are formulated for each cell, without momentum equations [19]. Yet, these models rely on a series of assumptions (e.g. constant temperature within the zone, require semi-analytical formulations based on the knowledge of the flow physics) which need to be considered when assessing the relevance of the predictions.

Computational fluid dynamics modelling divides a DSF system into a number of cells, where for each cell at least three conservation principles (mass, momentum and energy) must be satisfied [30]. Partial differential equations representing these conservation principles (Navier-Stokes equations) can be numerically represented and solved by using finite difference or finite volume method. The second method is the most common method for discretization, except very few researches such as Han’s [31]. A certain number of researchers developed their own CFD code or software for thermal and air flow analysis of DSF [32,33], but most researchers in their studies use commercial or open-source CFD software packages such as OpenFOAM, Ansys FLUENT, Tas Engineering, COMSOL or Phoenics. In general terms, the numerical solution can be obtained using three CFD approaches: direct numerical simulation (DNS), large-eddy simulation (LES) and Reynolds-averaged Navier--Stokes (RANS) equations simulation with turbulence models [34].

While DNS has not been used for modelling flow inside the DSF cavity, LES [35,36] has been adopted by some researchers who obtained excellent fit with experimental data, but none of them included solar radiation models [37,38]. Numerical results provided excellent statistics about turbulence quantities, which has been used later as a validation tool by other models of lower accuracy.

The selection of a proper RANS turbulent model for the characteristic flow inside the cavity determines to the greatest extent the accuracy [39] of thermal and fluid dynamic simulation when this approach is chosen. Two-equation turbulent models are the most used category of models for building related researches, because they offer a good level of accuracy along with satisfactory computing time [39]. Among them renormalization group k-ε (RNG k-ε) is the most applied because it showed a very good performance in modelling naturally ventilated DSF [40]. In several studies, there was no need for the introduction of turbulence models, due to examination of laminar flow inside naturally ventilated cavities [41]. Besides turbulence models, other components in a CFD model that influence the level of confidence in the results and computation time are the pressure-velocity algorithm, the type of computational grid, the uncertainty in boundary conditions, and the radiation model.

The level of confidence in numerical simulations and in CFD models can be determined through an experimental validation procedure, but only a small number of CFD studies have validated both thermal and airflow (velocity) field, while most studies rely purely on the simulation or have validated only thermal part of the model.

The main strength of CFD analysis is its ability to accurately simulate velocity, temperature and pressure field from which detailed information about thermal and energy performance of DSF can be extracted, though this comes at the cost of high computational time and resources needed. CFD analysis is usually employed for the process of optimization or resolving design issues: finding optimal cavity depth, materialization of DSF elements, selection of shading system, glazing type, airflow path and examination of flow around venetian blinds. Furthermore, CFD can assess specific parameters such as convective heat transfer coefficient between the DSF surfaces and ventilated cavity. The results from CFD simulations can be used for developing simple correlations for parameters that describe thermal and energy performance of DSF (e.g. correlation between Nusselt and Reynolds/Rayleigh number) [42–44].

3.2. Experimental analysis

The first experiments that can be linked to phenomena occurring in DSF systems were carried out in the middle of the XX century and were intended for a better understanding of buoyancy induced flow between vertical opaque parallel plates [45,46]. These experiments were performed in a laboratory where the temperature or heat flux of bordering surfaces was controlled, investigating the turbulent behavior of the flow and not the overall thermal and energy performance of the system. Because a large number of quantities were monitored with the high spatial and temporal resolution, the results from these studies were later used as validation tools for more recent CFD models of DSFs [37,42].

Experimental investigations can be divided into natural and controlled, depending on the possibility to control the surrounding environment. In natural experiments, the (full-scale) model of the DSF is exposed to a real outdoor (and indoor) transient environment, while in controlled experiments the outdoor conditions are replicated, where in the most cases only the thermal environment is controlled. Quite a few experiments were performed in both thermally and radiative controlled environments [16,43,47] and, to our best knowledge, no experiment was ever performed at controlled wind conditions. Usually, in these types of experiments, parametric analyses are done in steady state conditions and by deliberate variation of parameters such as physical properties of DSF (cavity depth or venetian blind angle) or boundary conditions (incident solar radiation or outdoor temperature).

The thermal environment in a DSF is usually monitored by measuring surface temperatures of glazing and shading devices, the temperature of the air in cavity, as well as the temperature of all the other surfaces and volumes that are part or have an influence on boundary conditions. The air cavity measurements require the greatest attention when it comes to the complexity of the measuring system due to non-isotropic features of the flow and the air temperature in the cavity, where several vertical and horizontal temperature profiles need to be monitored. In general, temperature sensors need to be shielded against direct radiation and in some situations ventilated to avoid that the radiative heat absorbed by the shield affects the measurements [48]. These protection measures may reduce experimental error, but at the same time they may represent obstruction to the air flow in the cavity, and more in general a perturbation of the thermal field around the measurement point.

The fluid dynamics behavior can be monitored by three main classes of techniques: bulk airflow methods; direct velocimetry; and non-intrusive velocimetry.

Bulk airflow methods determine bulk airflow rate inside ventilated cavities by measuring either the pressure loss across the cavity or by tracer gas technique. In the pressure difference method, airflow rate is estimated based on the pressure difference between the surface pressure at the opening and referent pressure inside of DSF, or across the cavity, where incense sticks can be used to judge the airflow direction [49]. This method is not suited for naturally ventilated cavities because the driving forces of the flow are usually weak. Such a method, moreover, requires that the pressure loss across the opening is previously calibrated against another measurement method of the airflow rate, or that the coefficient of discharge for the opening is simulated/measured experimentally. In the other class of methods, a tracer gas (usually carbon dioxide, CO_2 or sulfur hexafluoride, SF6) is monitored inside the cavity, where constant injection method (CIM), decay method (DM) and constant concentration method (CCM) could be used for evaluation of bulk airflow. CIM is probably the most used method by researchers, but generally all tracer gas methods are challenging for airflow measurements in naturally ventilated DSFs, due to the assumption of good mixing inside the cavity. In naturally ventilated DSFs, it is hard to achieve this because the flow is driven by weak forces and it is highly fluctuating. Large measurement error is expected there, when a significant amount of tracer gas is dispersed, and this can happen due thermal and velocity heterogeneities in the gap, insufficient mixing and variability of outdoor conditions [50].

The amount of information and its complexity that it is delivered through direct velocimetry vary from the most basic one, where only one bidirectional anemometer can be used for evaluation of bulk airflow, to the most advanced such as the velocity profile method. The velocity profile method ensures the airflow rate estimation, but also gives an indication of velocity distribution inside the cavity. Anemometers should be placed along several heights in the cavity in order to provide both horizontal and vertical velocity profiles. The accuracy of measurement needs to reach a tradeoff with the desired amount of information, because anemometers also represent an obstacle to the flow and a large number of these sensors in the cavity may significantly alter the flow. However, these methods are suitable for long term measurements and can therefore be very useful when infield investigations are carried out.

Non-intrusive velocimetry technique employs optical/acoustic methods for particle tracking upon which asses velocities, such as laser Doppler (LDV), particle image (PIV) or ultrasound velocimetry (USV) [51]. The first method allows the velocity to be measured only at one point, does not disrupt the flow and requires one initial fast calibration before measurement. Poor signal to noise ratio and consequent large measurement error that can be caused by attenuation and reflection of the signal inside the cavity [52], together with the need for a relatively complex instrumentation that is hard to use outside a laboratory, limit the application of this technique. The PIV method obtains instantaneous velocity fields by recording images of particles at successive times though the “trace” left by the fine particle used as a marker when illuminated by a monochromatic light. This method allows one to analyze the flow in the plane, and recent attempts are trying to expand this technique to 3D measurements. One of the main advantages of this technique is that it can measure a wide range of velocities, while costs and complexity of the experimental set-up is the main drawback. Different parameters affect the accuracy and reliability of this method, such as the characteristics of the particles (larger particles affect the flow, while smaller scatter insufficient amount of light, so a compromise needs to be reached [53]), non-uniform dispersion near the inlet, sedimentation, and induration of seeding material on the blades and casing of the fan [54]. Ultrasound velocimetry is another non-intrusive technique that has been recently applied in HVAC system and it is based on the interaction of ultrasonic sound with moving fluid [51], and seems a promising possibility for long-term monitoring in DSFs too, though applications of this method for DSFs have not been reported in the literature.

The radiative environment, or at least the radiation linked to short-wave sources like the Sun, is usually replicated in laboratory studies through the use of a solar simulator, i.e. matrix of multiple lamps with spectral properties close to natural solar radiation. Solar simulators are placed close to DSF and emit continuous light [55]. The calibration and verification of the solar simulator are very important, because asymmetry in the irradiating surface may occur [56]. The measurement of the incoming and transmitted irradiance is mostly carried out with pyranometers [57], though other sensors based on other photoelectric phenomena are also used even if their accuracy is lower. Pyranometer placed in the interior space behind DSF system is used for the measurement of transmitted solar radiation and solar gains, as well as the calculation of efficiency parameters (e.g. the dynamic insulation efficiency) [58]. In the case of measurement points behind DSF or shading, data from pyranometers has to be adjusted to the view factors calculated for the complex geometry in the DSF [48]. The longwave radiation flux (far infrared) exchanged with surroundings surfaces can be assessed with pyrgeometers [59].

4. Constructional features and thermal and fluid dynamics behavior of double skin façade

4.1. Literature data on experimental and numerical (CFD) studies

The comprehensive review of the scientific literature of studies that investigated the impact of different constructional features on the DSF’s performance is summarized in two tables which are reported in the Appendix for the sake of brevity of the manuscript. Table A.1 and Table A.2 are for experimental analysis and numerical (CFD) simulation, respectively.

We reviewed and organized nearly 70 studies in those tables according to the chronological order, we identified the main(s) constructional feature(s) investigated and the type of ventilation mode (mechanical or natural ventilation) of the cavity, and we summarized for each study some important features. While for experimental studies we focused on the experimental instrumentation and the type of control over the boundary conditions (e.g. an experiment in fully controlled conditions or under uncontrolled conditions), for numerical studies, we also focused modelling setting such as simulation tool, dimensionality, discretization method, turbulence and radiation model, grid type, as well as the presence of a validation procedure. CFD models can be validated against results from own experiments or against open literature experimental databases or results, or finally as intersoftware comparison, i.e. against other more precise/detailed numerical models. In the analysis of the validation procedure, we differentiated how the fluid mechanics part of the model is validated. If it is validated against measured velocity at several positions and heights or with the PIV technique, then we defined it as a CFD model with detailed validation (fully validated). If it is validated against bulk airflow rate measurements by pressure difference, tracer gas or any other bulk airflow method, then we indicated it as partially validated (since the spatial structure of simulated flow is not verified).

The detailed analysis of the literature data led us to summarize the pieces of evidence and established knowledge on how different characteristics affect the performance of the DSF, which we summarized in the following two sections 4.2 and 4.3, for mechanically ventilated DSFs and naturally ventilated DSFs, respectively. For the sake of completeness, we need to mention that in the past two decades a wide variety of novel types of mechanically and naturally ventilated DSFs has been investigated. The list below is intented to be a non-exhaustive overview of a few of such investigations, together with the performance improvement that the new solutions are targeting.

- DSF with solar chimney [49] (enhancement of natural convection),
- opaque DSFs [60],
- DSF containing PV elements: DSF with PV modules encapsulated in glazing (semi-transparent PV elements) [31,61], DSF with integrated PV blinds (PVB-DSF) [62] PV vent window with PV module installed on a louver that covers opening [63] (generation of electric power and reduction of transmitted solar radiation for DSF with semi-transparent PV elements),
- DSF with incorporated PCM materials: DSF with integrated PCM shading [64,65], ventilated windows with the PCM solar air heat exchanger [56], PCM layers in combination with PV integrated in DSFs [66,67] (absorption of excessive heat and reduction of the temperature in a cavity),
- a pipe-embedded double-skin façade (PDSF) with water as heat absorber [64] (absorption of excessive heat and reduction of the temperature in a cavity),
- Slim-Type Double Skin Window System [68] (easy to operate and reduction of SHGC in comparison to non-ventilated DSF and typical windows),
- triple glazed exhaust-air window (TGEW) [69] (removes excessive heat from the cavity)
- double-skin green façade (DSGF) [70] (reduction of the air cavity and surface glazing temperature),
- conditioned Trombe wall with installed venetian blinds [71] (enhancement of natural convection and reduction of the air cavity temperature).
- smart double skin facades that integrate Tungsten (W) doped Vanadium dioxide (VO_2) and a high absorbing aluminum nitride (AlN) coating. (SDSF) [72,73] (active control of the green-house effect in the cavity with the amplification in the winter and dampening in the summer period)

However, even if all or some of these developments might be interesting, and might add a large range of additional constructional features, we decided to keep the main focus of this analysis on conventional DSFs, as these systems still represent the largest type of DSF that are investigated and used.

4.2. Mechanically ventilated DSFs

In this paper, we classify under the category "mechanically ventilated DSF" all those configurations where the airflow is driven by one or more powered fans which transform the rotational kinetic energy of the blades into the translational kinetic energy of the flow. DSFs where the flow interacts (but is not induced) by the other powered elements such as operable vents, dampers, or louvers, and which are usually adopted to a module or control the airflow, are not considered as mechanically ventilated DSFs. Mechanically driven flow can significantly enhance some of the phenomena that affect the thermal behavior of such facades compared to a naturally driven flow, as well as lower the net heat transfer in comparison to conventional façade systems during the entire year, but especially in winter [74].

4.2.1. Geometric features

Dimension of the DSF cavity – Among all geometric properties of DSF, the influence of aspect ratio/cavity depth on fluid flow and heat transfer inside the cavity is the most investigated one. In the natural experiment where mechanically ventilated DSF with outdoor air curtain circulation was tested at high-noon summer conditions, it was concluded that mixed convection induced both by solar radiation and fan is strongly influenced by the aspect ratios (ratio between depth and height of cavity, D/H) [75]. Additionally, decreased aspect ratio leads to higher solar heat gains [68], both due to increased air temperature in the cavity and amplified multiple reflections.

Airflow path – We can distinguish five possible airflow paths in DSF: supply air (outdoor-indoor), exhaust air (indoor-outdoor), static air buffer (closed configuration), external air curtain (outdoor-outdoor) and indoor air curtain (indoor-indoor) airflow path [21]. For the indoor air curtain ventilation strategy, a further increase of the heat gain into a room can occur from the exhaust duct [76]. In the typical winter week and with the air supply ventilation strategy, preheating of delivered air can be significant during sunny days (15–25 °C) due to heat loss recovery and solar heat absorption. During periods without solar radiation temperature increase of supplied air is moderate (10 °C) [59]. Such air mass could be used for heating purposes in winter, thus leading to a reduction of the energy use for space heating or ventilation air heating [77].

Openings geometry - The size and shape of the inlet and outlet significantly affect the energy consumption of the fan. For example, when air circulates in outdoor air curtain mode, flow rises along with glazing opposite to the inlet, while lower velocities occur near the outer glazing. If the sharp edges and turns are present, a portion of the low-velocity zone near the inlet can be transformed into a recirculation zone, creating a pressure drop. Therefore, sharp edges should be avoided because they create a large pressure drop and behave like an obstacle to the airflow [38]. Attention should be paid to the inlet's width because it directly affects the average velocity within the channel [53], making it higher for narrower cavities. That is a consequence of the principle of mass conservation, based on which extracted airflow from the cavity does not change considerably either with dimensions of the air inlet or with the shading system's position.

Shading type and position –The heat transfer by radiation is dominant over convection and conduction for most environmental conditions and DSF configurations. It is found that the transmitted solar and exchanged long-wave radiation prevails over convective heat flux [58] and therefore the most important structural parameter in controlling thermal and fluid mechanics part of the double skin façade is, when installed in the cavity, the shading system. There are various types of shading systems installed in the DSF cavity, where the most common are vertical louvre, venetian and roller blinds. The velocity fields are highly complicated [64] with an integrated shading system in the cavity, with sometimes accentuated three-dimensional patterns that cannot always be ignored by the assumption of two-dimensional flow [54]. However, due to the higher surface roughness and frictional drag, the velocity field is more complicated in cavities with installed louvre and venetian blinds than in roller (screen) blinds.

Most studies on mechanically ventilated DSF analyzed the influence of venetian blinds on thermal performance, while other types of shading systems are less explored. Venetian blinds allow a greater flexibility in the management of the cavity thermal gain, as a different, dynamic surface can be exposed to the solar radiation, hence it is a more interesting solution when it comes to modulate the thermophysical and fluid mechanical behavior of the system.

The shading position has a large influence on air velocity distribution in the cavity. In the case where both the channels created by shading have different widths, velocity will naturally be higher in narrower channels, unless very different glazing types are used on the indoor and outdoor skin. When the shading is closer to outer glazing, the solar heat gains will be lower, while for the opposite situation, the temperature of the inner glass surface will be highest, which is preferable when the outdoor temperature is significantly lower than indoor [78].

Slat angle – Different properties of the shading system such as thermal and optical properties, position, as well as slat angle influence the thermal behavior of DSF. However, if it is a shading system with built-in slats, the most significant parameter in the control of the heat transfer is slat angle. For example, when a DSF system is exposed to solar radiation, the slat surfaces have usually higher temperatures than glazing and the air inside the cavity. These temperatures and temperatures of other structural elements of DSF can be primarily controlled through the slat angle and secondarily through the airflow rate [79]. The tilt angle of slat influences to the largest extent radiative heat transfer, which is a very important fact during the high-irradiation periods [78].

For a typical summer situation, when the slat and the incidence angle of solar rays are lower than 60° and 45°, respectively, transmitted solar flux is higher than exchanged long-wave radiation. The dynamic insulation efficiency, which is a measure to quantify the ability of a DSF to reduce the thermal fluxes entering an indoor environment, is independent of the ventilation strategy when the slat angle is higher than 75° [58]. The average velocity of the air in the middle of the channels created by venetian blinds increases as slats are getting closed, and in the case of fully closed slats (0°), the outdoor air channel and slats itself will have higher temperatures than if it is opened (90°) [53].

4.2.2. Materials properties

Glazing properties – Regardless of DSF type, solar heat gain into a building can be reduced almost by the order of the magnitude by the appropriate combination of optical properties of the inner and outer glazing [77]. For unshaded mechanically ventilated DSF, solar heat gain in a typical summer day can be reduced to double if the internal glazing is replaced with low-e glass and up to 40% if the transmissivity of outer glazing is reduced by 55% [80]. Other dedicated analyses investigating combinations of different spectrally selected glazing solutions have not been found in the current literature.

Therefore, in warm climates, it is not recommended to have a low aspect ratio (<0.1). Firstly, due to the merging of thermal boundary layers in a long channel and increased air temperature and secondly, due to decreased optical losses and increased multiple reflections in the thin cavity. On the contrary, this may be the preferred configuration for cold climates since higher solar heat gains and air temperature in the cavity are desired.

Radiative surface properties of shading system – The heat transfer by radiation is the main driver of the thermal performance of DSF, and therefore the radiative properties of the shading system play an important role. However, only in the last few years several numerical studies have specifically investigated this aspect. Increased emissivity of the front surface of venetian blinds reduces transmitted heat flux into the interior environment [58], while the thermal performance of DSF can be further enhanced, considering the cavity as a device to capture solar energy, when the absorptivity of the back surface of venetian blinds is increased, which reduces double reflection towards indoor [12].

Thermal properties of the shading system – High thermal capacity materials incorporated in the shading devices, such as PCM materials or water [56,64,81,82], can play an important role in controlling heat processes in DSF. However, the application of this technology has been limited only to naturally ventilated DSF. It would be interesting to see how mechanical flow can promote the release of the stored heat during night-time when external conditions do not favor (low wind speeds) [65]. What is the coupled effect of PCM and mechanical flow on the thermal performance of DSF in ventilation modes other than outdoor air curtain?

4.2.3. Airflow rate

In summer, a solar energy absorbed by DSF elements can be reduced efficiently by mechanical ventilation. In particular, SHGC can be reduced by one-third along with the temperature of outer glazing and installed PV panels with the right combination of the forced airflow velocity and cavity depth (e.g. 5 m/s and 200 mm [61]). However, one has to be careful, because the potential prevention of overheating can be overshadowed by operational costs [12]. Increasing the airflow rate, clearly, does not influence the transmitted solar radiation, but it reduces long-wave radiation exchange and increases dynamic insulation efficiency [58,83]. However, even the very high airflow rates may not be sufficient to reduce the overheating of the façade during the very warm weather in typical south-European climates. The only way to avoid this is to carefully plan the shading device, the glass type, and to adapt the airflow path [83]. From the point of the heat transfer, a key role is played by the fluid-dynamic characteristics of the flow, i.e. whether it is fully developed or is it still in the thermal and hydrodynamic developing phase. In a study where mechanically ventilated DSF with outdoor air curtain circulation was tested in a climate simulator without artificial sun [43], the flow was undeveloped in both senses for all environmental conditions (air temperature near inlet varied between 3 °C and 7 °C) and airflow rates (low, medium and high). Hence, heat transfer coefficients were found to be relatively higher, than it would be the case if the flow was developed. In typical summer conditions, circulatory motion with upward directed flow close to internal glazing and downward directed flow close to the opposite side has been observed [75], especially when the outer skin has low or little thermal resistance. These patterns create additional pressure drops and consequently increase the operational costs of DSF [80]. Therefore, in order to efficiently control the thermal performance of DSF, fan capacity needs to be designed based on pressure drops created by different structural elements of DSF [43].

4.3. Naturally ventilated DSFs

Because of the intricate nature of the flow and uncertain predictability of thermal, optical, and fluid mechanical behavior of naturally ventilated DSF, this type of DSF has been more studied than mechanically ventilated. However, some general conclusions can be drawn about performance, flow characteristics, and driving forces behind flow in naturally ventilated DSF. This type of DSF is a less recommendable choice for warm climates characterized by high irradiation levels, because structural elements of DSF can become hot (up to 70 °C) which can lead to overheating [84] and damage of delicate components like shading motors [85], while naturally induced airflow may be too modest to be used to remove the (solar) heat collected by the structures of the DSF. Therefore, the strengthening of naturally induced convective flow and heat transfer is desirable in periods with a high outdoor temperature and irradiation, with high Rayleigh number of the flow that ranges from 10^3 to 10^5 [31].

In several studies on the buoyancy-induced flow between two vertical parallel plates [6,41,86,87], circulation (bidirectional) flow with upward acceleration near the heated side has been observed along with downward deacceleration near the opposite side. This pattern is followed by the existence of a vortex in the central portion of the cavity. The most intensive fluctuations of velocity and temperature correspond to this cavity region, producing lower wall temperatures in this area [37, 88]. For a similar configuration where the central part of one plate is heated with constant heat flow, a recirculation zone appears at the outlet near the colder surface with the property that its size increases with Rayleigh number [41]. More unsteady vortices in the corners of the channel have been observed, too [32]. If the channel is non-uniformly heated from both sides [38], two plumes driven by buoyancy appears. This is opposite to the case where the channel is heated from one side only and where only one plume appear. It can be concluded that a channel heated non-uniformly from both sides generates a larger mass flow rate and more vigorous mixing than in a channel heated from only one side.

A common assumption in naturally ventilated DSF is that flow inside the cavity is buoyancy-driven [89]. However, several recent studies show that wind dominates as the driver of the mass flow rate [33,90]. Through CFD investigations [91] it has been shown that free-stream wind can be amplified to 1.8 times in the corridors of story-high DSFs, which makes this system especially convenient for wind energy harvesting by incorporating wind turbines in corridors. Both the buoyancy and wind as driving forces are investigated in the validated CFD research [90], where DSF with outdoor air curtain ventilation mode is subjected to four typical conditions. The complicated and nearly isothermal flow pattern with several recirculation zones characterizes the situation where the wind (regardless of wind pressure orientation) is more dominant than buoyancy. On the contrary, when buoyancy is dominant over the wind, circulation is weak with a temperature gradient that can be amplified if the wind pressure is opposed to buoyancy.

However, in addition to the general characteristics that are recognizable, there are many more unknowns, which led us to appropriately design the ventilation strategies, geometrical configurations, materials, and layers in order to provide the best condition to remove excessive heat from the cavity when desired [68].

4.3.1. Geometrical features

Dimensions of the DSF cavity – The height of the DSF is a very important factor as it enhances the stack effect and accelerates airflow inside the cavity [92]. For that reason, multi-story and shaft-box facades are more suitable for natural ventilation and preferred over the box window and corridor type facades [2]. During the cold season for supply ventilation mode, air velocity in the cavity is approximately proportional to the height of the DSF and roughly inversely proportional to the depth of the cavity. The temperature of the supply air, i.e. the air that leaves the DSF's cavity, is inversely proportional to cavity depth as well [93]. Some studies support the claim that a narrower cavity accentuates the natural flow inside the cavity. Others [94] emphasize that cross-sections of DSF should not be too shallow due to heat diffusion from hot surfaces and the consequent possibility of overheating. If DSF needs to deliver cold air, the channel width should not be larger than 0.6 m, while if it needs to provide warm air, then the width needs to be lower than 0.2 m [92]. With a reduction of aspect ratio, the transition from laminar to turbulent flow shifts higher and flow has a shorter entrance path. For turbulent flow, convective Nusselt number and local heat transfer coefficient increases when the aspect ratio increases, while for laminar flow, the opposite behavior is observed [86,87]. The length of the single recirculation zone that occurs at the outlet decreases with increasing aspect ratio [41].

Considering tilted (i.e. not perfectly vertical) DSFs, it can be said that the maximum heat and airflow rate occurs for the perfectly vertical channel. Tilting one side of the channel leads to a reduction of the Nusselt number and of the airflow rate [95]. In the same study, a recirculation zone near the outlet is observed, which increases in size with increasing positive tilt angle. Unconventional geometric configuration of DSF like this can reduce solar heat gains by self-shading and reduction of incoming solar radiation. However, according some researchers [94], if the adequate distribution of outlets is not provided, this configuration can lead to trapping of hot air in certain regions of the DSF.

Airflow path – Different airflow paths significantly influence the solar heat gain coefficient when the shading is not lowered [68]. In summer conditions, and with the absence of solar radiation, the closed configuration of the cavity is preferred because of low average temperature. In the presence of solar radiation in summer, outdoor air curtain ventilation type is a more efficient due to enhancement of stack effect and consequent lower transmitted heat gains and cooling load [96]. More advanced concepts have been proposed where a triple glazing divides the cavity in two separate elements. The shading device is placed in the outer zone through which air circulates in exhaust mode, while inner zone is closed. This configuration can effectively trap and remove the heat accumulated in the cavity during cooling periods with high outdoor temperature and irradiation and according experimental campaign it increases the temperature of the exhaust airflow [69]. A similar concept that uses inner closed zone and outer zone in the outdoor air curtain ventilation mode without installed shading device is proposed by Koo [97]. Experiments showed that natural ventilating of outer zone reduces SHGC and temperature of the cavity; however, at a significantly lower level than in the case of the previous configuration. In winter conditions, both with solar radiation and without, closed vents are recommended due to the higher average temperature of the cavity. Ventilation is not recommended as it lowers the air cavity temperature [84]. Otherwise, if it is necessary to provide fresh air during cloudy and cold weather, passive preheating of air in supply ventilation mode may not be enough [93].

Openings geometry - The size and arrangement of the openings and the cavity width significantly impact the overall performance of the DSF [98]. For typical summer conditions in very hot climates [99], the opening size has a more significant impact on the cavity's air temperature than cavity depth when the DSF is operated as an outdoor air curtain. An increase in the cavity depth leads to a rise in the cavity's temperature, while a larger opening size leads to the opposite situation. These two factors influence less the air velocity. For DSF consisting of both venetian blinds and high thermal-mass elements, larger openings area leads to stronger buoyancy flows [71]. The joint influence of cavity depth and opening size is very complicated and non-optimal dimensions can reduce to a great extent the naturally induced airflow in air supply ventilation mode in typical summer conditions [100].

Automatically controlled or manually controlled dampers and vents on the openings have been commonly used in naturally-ventilated DSFs to regulate and control the airflow to enhance the performance of the DSFs – i.e. reducing or suppressing the airflow when unwanted, while enabling it when required by the planned operational mode A comprehensive review on how dampers, vents, louvres, and any other controllable device impact on the airflow in terms of pressure drops for the naturally-induced flow would probably require a long list of individual cases, which is outside the scope of this paper. However, it is herewith important to point out that the use of such devices has been a practice in DSF design with several real-word implementations [101].

Velocities near openings are greatest because air is forced through the smaller area [44], and heat transfer to the inner side of DSF near the inlet is enhanced due to this amplified inflow of buoyant jet [102]. High intake speeds up to 1.6 m/s are possible on a typical summer day without wind [85], causing noise and the suction of dust. Through experimental analysis [86], the effect of entrance bell-mouth shape on buoyancy induced-flow is investigated for the case of vertical parallel plates set in outdoor air curtain ventilation mode. This type of inlet has found its application in practice due to round ends that can control the inlet disturbances more easily. Experiments showed that entrance bell-mouth shape leads to a delayed start and the end of the transition to turbulence and weaker disturbances, heat transfer, and velocity intensities, in the laminar and transition region. In a similar fashion, recessed regions at inlet and outlet along with rounded corners at walls increase mean velocity by one quarter at the middle of the passage of a corridor type DSF [103,104].

For naturally ventilated DSF, the position of the openings plays important role in the control of the heat transfer. Due to natural tendency of buoyant air to move vertically upwards, it is highly preferred to have openings located at the top and bottom of DSF, unlike for example lateral openings. If the wind is considered as a driving mechanism, central-placed (front) opening is preferred beside lateral openings, because this arrangement is less dependent on the wind direction. For normal winds, this configuration amplifies the airflow and makes a more uniform rate in the cavity, making that position especially effective for enabling natural circulation [105,106]. DSF naturally ventilated reduces overheating and amplifies airflow rate when approaching wind direction is normal to the surface of the DSF [2]. Placing louvers on the openings can significantly assist naturally driven flow, where a small change in the shape, position and inclination of louvers can enhance natural ventilation considerably [107]. If the air velocity is not strong enough to reach deeper in the cavity, louvers should be placed at the top of inlets so that they can direct air movement [94]. Open horizontal and vertical joints in ventilated facades can be used as well to induce more effective airflow, reducing heat transfer in this way [108].

Shading type and position – In naturally ventilated DSF heat transfer by radiation is even more dominant over convective and conductive compared to mechanically ventilated DSF, and therefore the most important structural element in controlling heat transfer is the shading device, just like in the mechanically ventilated DSF. The shading device reduces solar radiation and heat gains in the interior by absorbing heat and increasing the air temperature and the stack effect inside the cavity [2,109]. It separates the cavity into two vertical channels, where the type of blinds has a major impact on temperature and velocity distribution in the cavity [110].

Roller blinds can be assumed airtight, so there is no exchange of mass between two cavities. Airflow is less effective in extracting heat from roller blinds than from louvered blinds due to higher roughness and more contact of the latter type of shading device. Louvered blinds reduce the airflow rate compared to a roller blinds, but the overall velocity profile stays the same [44]. Additionally, horizontal louvers enhance stronger buoyancy and higher airflow compared to vertical louvers [109]. The presence of venetian blinds has little effect on the convective heat transfer coefficient at glazing surfaces [111].

The shading position (distance from the inner or the outer glazing) leading to optimal energy behaviour can only be found considering the different external conditions and specific performance goals. In general it is possible to see that the best position is similar in both naturally and mechanically ventilated DSF, with a preference of placing the shading closer to outer glazing when the outdoor temperature is significantly lower than the indoor temperature, and next to inner glazing in the other case [2,98].

Slat angle – Natural convection is complex and sensitive to an incident angle of direct solar radiation on slat [33] and generally is enhanced by the increment of slat angles [71,112]. Slats placed in open positions (0°∼30°) cause obstruction to the airflow in the cavity, while in a vertical position, drag in flow is reduced [2]. If slats are opened (0°), the two channels' temperatures approach each other, indicating higher interaction between them. For almost fully opened slats (15°), the temperature of the inner channel will be higher. The opposite situation happens when slats are nearly or fully closed (60°∼90°). In addition to this, heat fluxes to indoor can be reduced to 85% of incoming energy, and the blinds' temperature becomes higher [113]. The slat angle mainly influences the inner glass's surface temperature due to multiple reflections and absorption processes. However, this influence is additionally dependent on the shading position and aspect ratio of the cavity, as closing the blinds enhances heat transfer and absorption and reflection of sunlight [98].

4.3.2. Materials properties

Glazing properties – The effect of glazing radiation properties on thermal performance and fluid flow inside the cavity is even more accentuated for naturally than for mechanically ventilated DSF because these properties mainly determine glazing temperature, which represents a main driver of naturally induced fluid flow. For enhancement of the buoyancy induced flow, external glazing should be highly transparent, allowing high heat gain into the cavity [2]. However, suppose intensive heat transfer by radiation within the cavity is not preferred, like in hot summer conditions. In that case, it can be reduced by installing a low-emissivity glass [40] or other solutions with lower solar transmittance (e.g., PV glazing with low e-coating [31]), including smart, dynamic layers [73], where transmissivity of glazing decreases with increasing the ambient temperature [72]. PCM materials (mainly paraffin) can be applied on the inner façade to extend the ventilation period for several hours after sunset, making them potentially usable the DSF as a supply for fresh air not only in diurnal but in a nocturnal period as well [114]. For warm and dry subtropical climates, the two skins' thermal resistance is not crucial, and single-pane clear glass with a thickness of 6 mm is recommended for both sides with an optimum transmissivity of glass should lie between 0.7 and 0.9 [98].

Radiative surface properties of shading system – The size and the emissivity of the slats influence the naturally induced flow inside the cavity [98]. If the emissivity of the shading system (front surface) increases, the globally absorbed solar heat flux is reduced, and buoyant flow is enhanced inside the cavity. Consequently, the surplus heat is removed by the flow, and the cooling load is reduced [115]. However, the shading system's radiative properties do not influence only the thermal behavior of DSF; daylighting performance is highly determined by it as well, when the optical properties are analyzed in the visible spectrum. Therefore, one should be very careful in choosing the shading system's radiative properties, as improving thermal performance can lead to deterioration of daylighting performance and vice versa [98].

Thermal properties of the shading system – Adding heat capacity to the shading device (e.g. PCM integrated in blinds [64]) may reduce the outlet and air cavity temperature in summer conditions compared to conventional aluminum venetian blinds with no significant difference in comparison with ambient temperature [65,116]. Under this case, excess heat in the cavity is absorbed by the PCM layer, making the convective heat transfer in the cavity reduced, the airflow more stable and the exchange of long-wave radiation from high-temperature surfaces lower. It was also shown that the air temperature in the cavity is highest when the blinds with PCM are close to the external glazing, while it is opposite when it is placed closed to the internal glazing [117]. DSF with venetian blinds that use water as a cooling medium in embedded pipes is able to significantly reduce the temperature in the cavity (around 29 °C) [118], accumulated heat and peak heat transfer during summer days with high radiation compared to the traditional ones. However, they are not effective when the DSF is exposed to low irradiation levels (e.g. toward the north on the northern hemisphere or at night [119]).

5. Conclusive remarks: current knowledge, knowledge gaps, and possibilities for further research

The analyzed experimental and numerical studies provided a heterogeneous range of information and current knowledge on how the features of a DSF lead to different thermal and fluid mechanics behaviors. We tried to organize such current know-how to explicit the link between material properties and geometrical properties and DSF's performance.

The shading system represents the most influential structural element in controlling the thermal behavior of both naturally and mechanically ventilated DSF. Venetian blinds represent the most applied and investigated type of shading system, due to theirs flexibility in managing solar heat gains by changing several of its characteristics. Among the different properties of venetian blinds, the slat angle for both types of DSF plays a crucial role because it efficiently controls transmitted solar radiation. Glazing represents the second most influential structural element. However, this element's contribution is not in the same order of magnitude as the slat angle. In naturally ventilated DSFs, the influence of the glazing properties is generally more significant than in mechanically ventilated because glazing temperature drives buoyancy in the cavity.

For the same reason, the shading system's radiative surface properties may be significant in naturally ventilated DSF, though not with the same order of magnitude as the glazing optical (and to a lower extent, thermal) properties. In mechanically ventilated DSFs, the airflow rate is a parameter in the same range of relevance as the glazing properties. In the conventional shading system such as aluminum venetian blinds or roller blinds, the thermal properties are rather insignificant, but if more complex shading devices are installed (e.g. shading with phase change materials or high-capacity materials, or combined with systems that provides a heat sink effect in the shading device, the effect of the thermal properties of the blinds in some situations can be in the same order of magnitude as the slat angle.

The airflow path, the dimensions of the cavity, and openings geometry represent factors closely related, and they need to be carefully coordinated to optimize the thermal performance of DSF. However, individual adjusting of these factors may not lead to significant performance improvements, though they can lead to severe performance deterioration if they are not adequately designed. Both wind (when present) and buoyancy play an important role in driving airflow inside the DSF cavity, yet the wind makes the flow pattern more complex. What drives the flow to a greater extent depends on climatic conditions (ambient temperatures, dominant wind intensity, and orientation) and the DSF configuration (opening size and position, cavity depth, glazing,

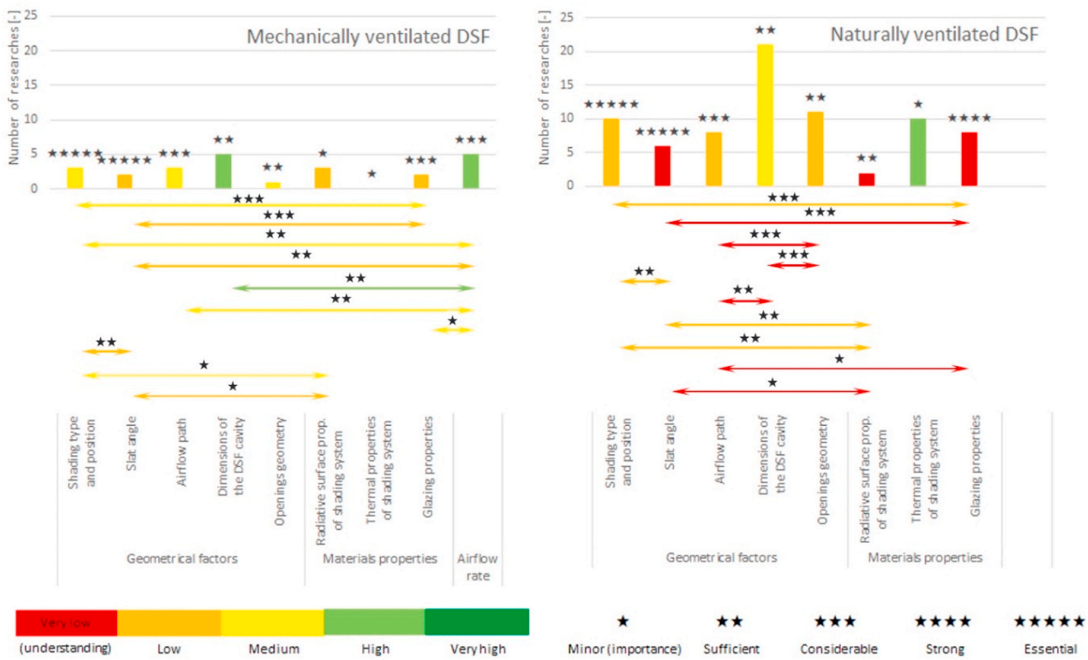

Fig. 4. A summary of the current understanding of the impact of structural elements and their interactions on the thermal and fluid dynamics behavior of DSFs.

and shading properties). However, if the conditions are so that both factors are present (e.g. for an outdoor air curtain façade), the wind will likely be a more dominant mechanism.

There are relevant unexplored or underexplored links regarding how different arrangements of structural parameters in conjunction with boundary conditions influence the thermophysical and fluid mechanics processes in DSF. These unknowns are accompanied by uncertainties and limitations regarding methods and techniques used for the investigation of these phenomena.

We can see that wind-induced flow is usually dominating over buoyancy-driven flows, however the exact balance of these two mechanisms, or the coexistence of buoyancy-driven flows and artificially (though fans) induced flows is mostly unexplored. There is a noticeable lack of numerical and experimental studies where the simulated flow is driven simultaneously by more than one mechanism. When it comes to wind-driven flows, the outside environment is usually not directly modeled, and therefore it is impossible to examine how different wind intensities and directions will influence the flow in conjunction with buoyancy.

We could summarize general cause-effect links between property families, property subcategories, and thermophysical and fluid mechanic behavior (Fig. 4). Usually, the influence of a single parameter at a time can be quite often explained and, to some extent, quantified, even if with different degrees of understanding. However, the combined and complex effects of more parameters together are almost never analyzed. For example, it is difficult to understand what is the effect resulting from two features that affect in an opposite way a certain performance, whether one or the other is dominant, and to what extent. Dedicated analyses investing the balance of effects between different driving forces and different constructional features would therefore give a more grounded understanding of these systems and thus support their optimization.

Studying experimentally the variation of two or more parameters at the same time require high control of the boundary conditions. Experiments with fully controlled thermal and radiative environments are however very rare as they require suitable indoor facilities. These analyses should be highly prioritized, and dedicated experimental methods developed, to provide evidence and quantifications of the effects of multiple features on the thermophysical and fluid mechanical behavior of DSFs. Experiments in controlled environments can also provide invaluable data for numerical models' validation, thus contributing to the possibility to study more comprehensively the complex interactions among different constructional features in a numerical way.

Best practices and recommendations for CFD models targeting typical situations and configurations of DSF are currently missing, and a comprehensive, systematic review of CFD modeling that gives recommended strategies (in terms of suggested turbulence and radiation model, solution algorithm, grid type, dimensionality, etc.) would be definitely beneficial to enhance the robustness of advanced numerical studies of DSF systems.

Declaration of competing interest

The authors declare that they have no known competing financial interests or personal relationships that could have appeared to influence the work reported in this paper.

Acknowledgements

The activities presented in this paper were carried out within the research project "REsponsive, INtegrated, VENTilated - REINVENT – windows", supported by the Research Council of Norway through the research grant 262198, and partners SINTEF, Hydro Extruded Solutions, Politecnico di Torino, and Aalto University.

We would like to thank the anonymous reviewers for the excellent cooperation in the review process, which helped us improve the final version of the manuscript. Finally, we would like to thank our colleage Dave Collins for proofreading the manuscript and improving its readability.

Appendix

Table A.1
Experimental studies on thermal and fluid dynamics behavior of DSF

Place	Year	Examined configuration	Examined constructional features/ quantities	The description	Type of experiment	Controlled environment	Thermal field	Velocity field	Other important variables
Queens Mary College, University of London, England and L'Ecole Nationale Superieure de Mecanique et d'Aerotechnique, Poitiers, France [52]; [42]	1989	Vertical parallel plates channel naturally ventilated (buoyancy only)	Two heights: 2.0 m and 2.5 m, Two widths: 0.5 m and 0.2 m, Three temperature differences: 32K, 46 K and 61 K.	The doctoral dissertation that investigates turbulent natural convection in rectangular air-cavities which can be suitable for DSF under certain conditions. Valuable information on correct experimental set-up and common issues. Final results from the study served as a validation tool for more recent CFD models.	Controlled	Radiative: no Thermal: yes Wind: no	Thermocouple (25 µm chromel-alumel) for measuring surface and air cavity temperatures	Laser Doppler anemometer	–
Yamaguchi University, Ube, Japan [86]; [37]	1991	Vertical parallel plates channel naturally ventilated (buoyancy only)	Three different channel spacing (500, 100 and 200 mm), with and without bell-mounted inlet and three different heat fluxes on the heated wall (50, 100 and 200 Wm^{-2}).	Experimentally study of a flow between vertical parallel plates with valuable information on various turbulent quantities. Used as validation source for later studies on similar topics. Results from research applicable to DSF under certain conditions.	Controlled	Radiative: no Thermal: yes Wind: no	Thermocouples for measuring surface (100 µm chromel-alumel) and air temperature in the channel (25 µm chromel-alumel).	Laser Doppler anemometer	–
Imperial College, London, England [88]	1996	Vertical parallel plates channel naturally ventilated (buoyancy only)	Fluid dynamics and thermal behavior of air cavity with an aspect ratio of 28.6 and with a Rayleigh number of 0.83 $\times 10^6$.	Experimentally study of a flow between vertical parallel plates with valuable information on various turbulent quantities. Used as validation source for later studies on similar topics. Results from research applicable to DSF under certain conditions.	Controlled	Radiative: no Thermal: yes Wind: no	Thermocouples (75 µm chromel-alumel) for surface and air temperature in the channel.	Laser Doppler anemometer.	–
Technical university of München, Germany [75]; [110]	2002	Hybrid (buoyancy only)and mechanically ventilated DSF.	Three cavity depths: 0.3, 0.6 and 0.9 m. Different airflow rates: 0.06–0.6 kg/s. All experiments were performed at high noon for conditions with mixed convection.The height of the air inlet can be changed.	This experimental study provides the time and locally averaged heat transfer coefficients for mixed convection in DSF facades. Furthermore, it describes general features of the flow and its dependence on gap width and mechanical airflow rates.	Natural	–	Resistance thermometer for surface temperatures (PT100) and thermocouples (type K) for air cavity temperatures.	Impeller wheel (plate) thermal anemometers for measuring velocity of air in cavity.	Pressure difference method for measuring airflow rate. Venturi section for measuring airflow rate in ventilation duct. Pyranometer for measuring incident and transmitted solar radiation.
Catholic University of Leuven, Belgium [84]; [44]; [89]	2002	Mechanically and naturally ventilated DSF (both, buoyancy and wind) with	One-year measurement, where roller blind is activated when solar radiation	The doctoral dissertation of Saelens provides valuable information on thermophysical	Natural	–	Thermocouples (T-type) for measuring surface, air cavity and openings temperatures.	Not measured	Pressure difference and tracer gas method for measuring airflow rate.

(continued on next page)

Table A.1 (*continued*)

Place	Year	Examined configuration	Examined constructional features/ quantities	The description	Type of experiment	Controlled environment	Thermal field	Velocity field	Other important variables
		integrated roller blind.	exceeds 150 W/ m^2.	behavior of DSF from both numerical and experimental work, where both natural and field experiments were performed. Useful information about the correct experimental set-up that will minimize installation errors is provided along with a list of advantages and limitations of different methods for evaluation of the airflow (pressure difference, tracer gas and velocity profile method). Thermal behavior of DSF is described for two types of DSF, naturally and mechanically ventilated, for summer and winter period along with assumptions whether wind or buoyancy dominate naturally induced flow.					
Swiss Federal Laboratories for Materials Testing and Research EMPA, Duebendorf, Switzerland [12]; [33]; [76]; [120]	2004	Mechanically ventilated DSF with integrated metalized shading screen.	Mechanical airflow rate of 60 m^3/h. Several days measurement.	Mechanically ventilated DSF with integrated metalized shading screen were subjected to outdoor conditions and all-day measurements. Valuable findings on how to decrease solar heat gains are given.	Natural	–	Thermocouples for measuring surface, air cavity and openings temperatures.	Not measured.	Differential pressure airflow meter for measuring airflow rate in the cavity.
Waseda University, Tokyo, Japan [49]	2005	Naturally ventilated DSF (buoyancy only) with solar chimney	Different sizes of openings on top of the solar chimney with a different temperature rise of blinds.	Experimental study on natural ventilation behavior of reduced scale model (1/25) of the south-oriented facade with double-skin and a thermal storage space (solar chimney) above the DSF. Panel heaters used to simulate the temperature rise of DSF and its absorption. Results from experiments have been used for validation of CFD models.	Controlled	Radiative: no Thermal: yes Wind: no	Thermocouples for surface, air cavity, solar chimney and occupant space.	Not measured	Pressure difference distribution is measured at points in solar chimney relative to interior space.
Centre de Thermique de Lyon CETHIL, INSA Lyon, France. [53]; [58]	2006	Mechanically ventilated DSF with integrated venetian blinds.	Slat angles: 0, 15, 30, 45 and 60°. The shading system position: 5, 15 and 25 cm from the inner glazing.	In the doctoral dissertation of Safer, experimentally and numerically mechanical DSF is tested with external air curtain ventilation mode	Natural/ Controlled	Radiative: no Thermal: yes/no Wind: no	Not measured	Particle Image Velocimetry (PIV) technique for measuring velocity of air in cavity.	–

(continued on next page)

Table A.1 (*continued*)

Place	Year	Examined configuration	Examined constructional features/ quantities	The description	Type of experiment	Controlled environment	Thermal field	Velocity field	Other important variables
			The width of the inlet: 2 and 3 cm.	and integrated venetian blinds. The main influent structural parameters are recognized: slat angle, position of shading system, airflow rate, opening position, incident of the direct solar radiation and weather conditions. Valuable information and recommendations regarding the PIV technique are given. Characteristics of the flow in the cavity are given in response to slat angle, shading position, the width of the opening.					
Politecnico di Torino, Italy [83]; [78]	2007	Mechanically and naturally ventilated DSF (buoyancy only) with integrated venetian blinds.	Monitoring lasted for two years with different operating conditions: a) with and without venetian blinds; b) mechanical ventilation with the nominal air flow rate 50 m^3/ h; c) mechanical ventilation with an increased air flow rate 75 m^3/ h; d) natural ventilation with the filter on the supply opening of the air gap; e) natural ventilation without the filter.	An extensive measurement campaign is performed on the DSF connected with HVAC through exhaust ventilation mode during actual operating conditions in order to assess the energy and comfort performance.	Natural	–	Thermocouples for measuring surface, air cavity and openings temperatures.	Hot wire anemometer for air velocity in the cavity.	Tracer gas method for measuring airflow rate. Solarimeter for measuring incident and transmitted solar radiation. Heat flux meters for measuring heat flux through DSF element.
Loughborough University, England [47]; [6]; [113]; [115]; [109]; [99]; [112]; [111]; [98]	2007	Natural (buoyancy only) DSF with integrated venetian blinds.	Incident solar radiation: 187, 360, 540 and 715 W/m^2. Outside air temperature: 12, 20 and 30 °C. Slat angles: 0, 30, 45, 60 and 90°.	CFD model of natural DSF is developed based on the results from a controlled experiment in a climate chamber with a solar simulator. Interesting conclusions are found about the thermal and fluid dynamic behavior of DSF in response to the presence of shading element and tilt angle of its venetian blinds.	Controlled	Radiative: yes Thermal: yes Wind: no	Thermocouple (T-type) for measuring surface, air cavity and openings temperatures.	TSI air velocity transducers (omnidirectional) for measuring air velocity in cavity.	Pyranometer for measuring incident solar radiation.

(*continued on next page*)

Table A.1 (*continued*)

Place	Year	Examined configuration	Examined constructional features/ quantities	The description	Type of experiment	Controlled environment	Thermal field	Velocity field	Other important variables
Aalborg University, Denmark [48]; [102]; [90]	2008	Mechanically and naturally ventilated DSF (both, buoyancy and wind).	Three ventilation modes: 1 (outdoor air curtain), 2 (buffer zone) and 3 (air supply).The a irflow of 143 m^3/h was used as a supply in 3rd ventilation mode. Several days of monitoring.	Technical report as a part of the doctoral dissertation of Kalyanova provides information about thermophysical behavior of DSF with integrated both natural and mechanical ventilation mode based on several days of monitoring. Valuable information about the correct set-up for pressure difference, tracer gas and velocity profile methods are given. Conclusion on what drives more natural flow in the cavity is given.	Natural	–	Thermocouples (K-type), for measuring surface, air cavity and openings temperatures.	Hot sphere anemometers for measuring air velocity in cavity.	Pressure difference and tracer gas method for measuring airflow rate. Pyranometers for measuring incident and transmitted radiation. Ultrasonic anemometer for evaluation of wind velocity profile.
San Vendemiano, Treviso, Italy [121]	2010	Mechanically ventilated DSF with integrated venetian blinds	For different incident radiation and outdoor temperatures with an airflow rate of 40 m^3/h.	Paper presents validation of CFD model from experimental data obtained from a full-scale test room with DSF located in San Vendemiano (TV), Italy.	Natural	–	PT1000 temperature sensors for measuring air cavity temperatures. Resistance temperature detectors (RTD) for measuring surface temperatures of glazing and blinds.	Not measured	Pyranometer for measuring incident solar radiation. Automatic mini weather station.
Centre de Thermique de Lyon CETHIL, INSA Lyon, France [79]; [16]	2011	Mechanically ventilated DSF with integrated venetian blinds.	Airflow rates: 0, 200, 400 and 600 $m^3\ h^{-1}$. Slat angles: 0, 30, 45, 60 and 90°.	Full-scale experiment in climate chamber equipped with solar simulator provides information about the influence of airflow rate and slat angle of venetian blinds on the thermal behavior of mechanically ventilated DSF. Valuable information about correct experimental set-up in a controlled environment is given.	Controlled	Radiative: yes Thermal: yes Wind: no	Thermocouples type (T-type) for measuring surface, air cavity and openings temperatures.	TSI air velocity transducers (omnidirectional) for measuring air velocity in cavity.	Differential pressure airflow meter for measuring airflow rate in the cavity. Mobile pyranometer for measuring distribution of incident solar radiation.
Tsinghua University, Beijing, China [122]; [119]; [118]	2012	Natural (both, wind and buoyancy) DSF with integrated venetian blinds	Three different outdoor conditions: incident solar radiation, angle and outdoor temperature.	Paper presents the validation of CFD model based on field experiments on DSF model. It provides a database for validation of other more recent CFD models.	Natural	–	Thermocouple (T type) for measuring surface and air cavity temperature.	Not measured	Tracer gas method for measuring airflow rate.
University of Reims, France [41]; [95]	2012	Vertical parallel plates channel naturally ventilated	Different aspect ratios and modified Rayleigh numbers	Numerical results of the CFD model are compared with experiments carried out in the water.	Controlled	Radiative: no Thermal: yes Wind: no	Measured, but not analyzed, because water was used as working medium.	Particle Image Velocimetry (PIV) technique for deducing	Heat flux distribution was assessed based on temperature measurement

(*continued on next page*)

Table A.1 (*continued*)

Place	Year	Examined configuration	Examined constructional features/ quantities	The description	Type of experiment	Controlled environment	Thermal field	Velocity field	Other important variables
		(buoyancy only)	(between $2\cdot10^5$ and 4 and $2\cdot10^6$).	Simulation points to the patterns of the recirculation zone observed in the experiments.				streamline patterns.	along heating plate.
University of Technology Graz, Austria [123]	2014	Three types of naturally ventilated DSF (both, buoyancy and wind): naturally ventilated DSF with PV module and inner opaque facade, natural opaque DSF with solar collector and standard DSF design	Cross-comparison of thermal behavior via recorded surface temperatures of three different types of DSF for two summer days in Graz.	This study determines thermal behavior and airflow characteristics inside different types of natural DSF. Experimental campaign for one year was performed in order to validate the CFD model and to cross-compare the thermal behavior of these three types of DSF.	Natural	–	Pt 100 elements for measuring surface temperature of PV module and inner wall (DSF with PV module), surface temperature of thermal insulation and interior wall (opaque DSF) and surface temperature of interior glazing and interior wall (standard DSF).	Two hot wire anemometers for measuring velocity in the cavity of DSF with integrated PV modules	Automatic weather station.
University of Science and Technology of China, Hefei, China [71]; [124]	2015	Trombe wall naturally ventilated (only buoyancy) with integrated venetian blinds	Location of the venetian blinds (Z/m): 0.04, 0.05, 0.06, 0.07, 0.08, 0.09 and 0.10. Width of the air cavity (m): 0.18, 0.16, 0.14, 0.12, 0.10 and 0.08. Area of inlet/ outlet vent (m^2): 0.2 x 0.1, 0.3 x 0.1, 0.4 x 0.1, 0.5 x 0.1, 0.6 x 0.1 and 0.7 x 0.1.	The paper presents an experimental rig that was constructed and utilized to validate the CFD prediction.	Natural	–	Thermocouples for measuring surface and air openings temperature.	A kanomax A533-type anemometer for measuring velocity in the cavity.	Pyranometer.
Centre de Thermique de Lyon CETHIL, INSA Lyon, France [38]	2016	Vertical parallel plates channel naturally ventilated (buoyancy only)	Two examined configurations: 1) uniformly heated one side and 2) both sides heated with spatial periodicity 1/15 of the overall height with a heat input of 220 W/m^2	The experiment in the laboratory on the naturally induced flow between two vertical parallel plates provides recommendations on a preferred arrangement of PV panels that will reduce overheating of the cavity.	Controlled	Radiative: no Thermal: yes Wind: no	Thermocouples type (K-type) for measuring surface and air cavity temperatures.	Particle Image Velocimetry (PIV) technique for measuring velocity of air in cavity.	–
Building Physics Laboratory, İzmir Institute of Technology, Turkey [42]; [43]; [125]; [126]	2016	Naturally (buoyancy only) and mechanically ventilated DSF	7 experiments with naturally ventilated DSF with different Rayleigh numbers ranging from $8.59\cdot10^9$ to $1.41\cdot10^{10}$. [42] 18 experiments with mechanically ventilated DSF using perforated plates with two holes different in size: flow (low, medium and high) in combination with three incident solar	Several experiments on both naturally and mechanically ventilated DSF are performed in the laboratory in Izmir, based on which numerical models have been developed.	Controlled	Radiative: yes/no Thermal: yes Wind: no	Thermocouples (T-type) for measuring surface, air cavity and openings temperatures.	Not measured	Pressure difference method for measuring airflow rate. Pyranometer for measuring incident solar radiation.

(*continued on next page*)

Table A.1 (*continued*)

Place	Year	Examined configuration	Examined constructional features/ quantities	The description	Type of experiment	Controlled environment	Thermal field	Velocity field	Other important variables
			radiation. [125] 9 experiments with mechanically ventilated DSF: Three cavity depth (25, 32.5 and 40 cm) in combination with three airflow rates (low medium and high). [43] 12 experiments with mechanically ventilated DSF: two cavity depths (25 and 35 cm) in combination with three airflow rates (low, medium and high) and two radiation levels (around 185 and 350 Wm^{-2}). [126]						
The Hong Kong University of Science and Technology, China [106]; [105]; [104]	2017	Natural (wind only) DSF	Different incident wind angles.	A series of wind tunnel tests have been conducted to investigate the characteristics and related mechanisms of flow within the cavity of DSF integrated with a tall building model (1:150 scaled CAARC building model) at different incident wind angles.	Controlled	Radiative: no Thermal: no Wind: yes	No measured	60 Kanomax omni-directional anemometer probes for measuring velocities inside cavity.	–
Korea Institute of Civil Engineering and Building Technology, Goyang-si, Korea [97]	2017	Natural (buoyancy only) DSF in the laboratory. Both driving mechanism in outdoor tests.	Two different glazing configurations with and without ventilation (O–O mode) in the laboratory test. Thermal behavior of chosen configuration in outdoor conditions during several day measurements.	This paper proposes a configuration of the DSF that reduces SHGC without using a shading device, only by ventilating the outer zone of the cavity, while the inner zone is closed. Thermal performance is confirmed by the tests in the controlled environment and in the outdoor conditions.	Both, controlled and natural	Radiative: yes Thermal: yes Wind no.	Thermocouples for surface and air cavity temperatures	Not specified	Pyranometer. Indoor thermal comfort parameters (PMV and PPD).
The University of Nottingham Ningbo China. [64]; [116]; [65]; [117]	2017–2019	Natural (both, buoyancy and wind) DSF with integrated PCM blinds	Several days monitoring during hot summer days. Comparison with thermal behavior of standard aluminum DSF.	Experimental campaign during hot summer days in Ningbo where thermal behavior of small representative DSF element (1.05 × 0.95 m) has been analyzed. The influence of wind has not been analyzed. Data from	Natural	–	Thermocouples (K-type) for surface, and air cavity temperatures	Hot-wire anemometers for measuring velocity in the cavity	Meteo-station for monitoring outside conditions

(*continued on next page*)

Table A.1 (*continued*)

Place	Year	Examined configuration	Examined constructional features/ quantities	The description	Type of experiment	Controlled environment	Thermal field	Velocity field	Other important variables
				this campaign has been used for the validation of several CFD models.					
The Korean Institute of Construction Technology KICT, Ilsan, Korea [68]	2018	Natural (buoyancy only) DSF	Tree different configuration of slim-type DS window system has been subjected to the fixed incident solar radiation (around 500 Wm-2) and indoor (25 °C) and outdoor temperature (30 °C) in order to assess SHGC and temperature distribution in the cavity.	A novel type of DSF which reminds on the two double-glazed windows separated with the slim cavity was exposed to tests in the metering box and climate chamber with an installed solar simulator in order to assess SHGC and temperature distribution in the cavity. Results from experiments were used for validation of the CFD model.	Controlled	Radiative: yes Thermal: yes Wind: no	Thermocouples for the air cavity	Not measured	Measurement of SHGC according to KS L 9107 Test (Korean standard).
Universidade Federal de Ouro Preto, Brazil [60]	2018	Natural opaque (both, buoyancy and wind) DSF	Comparison of three days measurement between the wall with added external façade (opaque DSF) and standard wall without external layer.	The thermal performance of opaque DSF has been analyzed through a three-day measurement campaign and compared to the thermal performance of a one-skin wall. The influence of wind has not been analyzed. Results from the experiment served also for validation of the CFD model.	Natural	–	Thermocouples (K-type) for measuring surface temperatures	Hot wire anemometer for measuring air velocity in the cavity	–
Tongji University, Shanghai, China [70]	2018	Natural (both buoyancy and wind) DSF with green vertical greening system	Comparison of thermal behavior (air cavity, surface and indoor temperature) of DSF with vertical greening system and masonry wall.	Experimental summertime campaign on the thermal performance of DSGF of a 5-story administrative building in Shanghai.	Natural	–	Thermocouple (K-type) for surface temperature of outer vegetated skin, Temperature/RH smart sensor for air cavity temperature.	–	Automatic weather station. Equipment for indoor thermal quality assessment (globe temperature sensor and wind velocity sensor)
Hunan University, Changsha, China [62]	2018	Naturally ventilated DSF (both buoyancy and wind) with integrated PV blinds.	Comparison between ventilated and non-ventilated modes. Comparison of thermal performance between traditional opaque façade, and naturally ventilated DSF with integrated PV blinds.	This experimental research compares thermal behavior and electric performance of PVB-DSF with a traditional envelope element.	Natural	–	Thermocouples Pt100 for measuring glazing, PV cells surface temperatures and air duct temperature.	Hot wire anemometer for measuring velocity of air near inlet.	Pyranometers for direct and diffuse solar radiation. Output voltage of PV blinds.
La Rochelle University, France [59]	2019	Mechanically ventilated DSF	The volumetric flow rate across the airflow window has been gradually increased from 8 m^3h^{-1} to 48	The experimental campaign is performed in order to validate the numerical model and to investigate the thermal	Natural	–	Thermocouples (K-type) for measuring surface and air cavity temperatures.	The extracted airflow rate from test cell is assessed from air velocity measurements at the exhaust duct	Pyranometer and pyrgeometer measured total incident solar flux and exchanged

(*continued on next page*)

Table A.1 (*continued*)

Place	Year	Examined configuration	Examined constructional features/ quantities	The description	Type of experiment	Controlled environment	Thermal field	Velocity field	Other important variables
			m^3h^{-1} in order to investigate its effect on the thermal behavior of the window during a typical sunny and a quite warm winter week.	performances of a triple-glazed airflow window, by comparison to the convectional double-glazed window.				(hot wire anemometer).	longwave radiation flux. A cup anemometer and a weathervane measured the wind speed and its direction.
Huazhong University of Science and Technology, Wuhan, China [69]	2019	Naturally ventilated DSF with venetian blinds integrated into the switchable cavity.	Comparison of thermal behavior of triple glazed exhaust window and classic window along with validation of numerical study.	Experimental campaign on the novel DSF that is able to work in two modes (summer and winter) using switchable cavity were performed during two typical summer days in Wuhan in order to validate the numerical study.	Natural	–	Temperature sensors for measuring temperature of surface and air near openings.	–	Pyranometer for measuring incident radiation. Hot wire anemometer for measuring airflow delivered to the chamber (not installed in the cavity).
Brno University of Technology, Czech Republic [66]	2019	Naturally ventilated DSF with integrated PV cells and PCM material on the inner opaque side.	Two types of ventilated BiPV façade are tested: with and without PCM layer located behind the PV cells.	Experimental investigation of a novel combination of BiPV/PCM integrated in naturally ventilated DSF. The study does not contain specific information about used sensors.	Natural	–	Temperature sensors for surface and air in the cavity.	Sensor for velocity in the cavity.	Heat flux for measuring heat flow.
Yongin, Gyeonggi-do, Korea [40]	2019	Naturally ventilated DSF (slim type)	Cavity	This study analyzes the cooling energy performance of SDSW through field measurement.	Natural	–	Thermocouples for measuring surface and air cavity temperatures	–	Pyranometer for incident solar radiation. PMV meter for indoor space.
The University of Sydney, Australia [103]	2019	Naturally ventilated DSF (wind only)	Opening configuration (recessed regions, curved walls, converging and diverging passages)	Experimental research in a wind tunnel investigates mean flow characteristics inside the opening of a corridor-type DSF on a high building replica.	Controlled	Radiative: no Thermal: no Wind: Yes	–	Particle Image Velocimetry (PIV) technique for measuring velocity of air in the cavity.	Cobra multi-hole pressure probe for validating PIV technique.
Centre for Energy and Environment, Jaipur, India [61]	2020	Photovoltaic DSF naturally and mechanically ventilated	Cavity depth (50, 100, 150, 200 and 250 mm) and ventilation type (naturally and mechanically ventilated: 2, 2.75, 3.5, 4.25 and 5 m/s)	Comparison of experimental performance of naturally and mechanically ventilated photovoltaic DSF with outdoor air curtain ventilation mode during the typical cloudless day in a cooling period.	Natural	–	K-type thermocouples for inner surface of the PV panel and glass and the air cavity temperature	Hot wire anemometer for air velocity inside the cavity.	Pyrheliometer and two pyranometers for incident radiation and transmitted radiation. Automatic weather station. Conductive and radiative heat flux sensors.
Laboratoire de Genie Civil et geo-Environnement (LGCgE), Bethune, France [87]	2020	Vertical parallel plates channel naturally ventilated (buoyancy only)	Five different aspect ratios (5; 6.25; 8.34; 12.5 and 25) and four different temperatures (303 K, 313 K, 323 K and 342 K).	Experimental study of natural convection inside an asymmetrically heated open double vertical façade applicable to DSF under certain conditions. The intelligent way to make experiments with low investment.	Controlled	Radiative: no Thermal: yes Wind: no	Thermocouples for measuring surface and air temperature in the channel.	–	Heat flux sensors for measuring heat flow.

Table A.2
CFD studies on thermal and fluid dynamics behavior of DSF

Name	Year	Examined configuration	Examined constructional features/ quantities	Used tool	Discretization method and dimensionality	Turbulence model	Grid type	Validation	Solution algorithm	Radiation model	The description
Airflow patterns and thermal behavior of mechanically ventilated glass double facades [76]	2004	Mechanically ventilated DSF with integrated shading screen	Cavity	Flovent	Finite volume (2D)	RNG k-ε model	Structured (rectangles)	By own experiment: thermal part: yes dynamical part: no	SIMPLE	Spectral optical model	A procedure for spectral optical and a CFD modelling is described and simulated results are compared with an experimental investigation built in an outdoor test facility
Influence of glass properties on the performance of double-glazed facades [77]	2005	Naturally and mechanically ventilated DSF	Ten different combination of glasses with different values of reflectance, transmittance and absorption coefficient.	Ansys Fluent (version not specified)	Finite volume (2D)	Standard k-ε model	Structured (rectangles)	Not validated	Not specified	Not specified	In this research the influence of the glass properties on the thermal performance of DSF has been studied through the unvalidated 2D model of both, naturally and mechanically ventilated DSF without venetian blinds.
Natural ventilation performance of a double-skin facade with a solar chimney [49]	2005	Naturally ventilated DSF with solar chimney	Different height of solar chimney and size of the openings	Not specified	Finite volume (3D)	Indoor zero-equation model (low turbulence)	Structured (rectangles)	By own experiment: thermal part: yes dynamical part: incomplete	Not specified	Not specified	CFD analysis is carried out in conjunction with a reduced scale model experiment in order to evaluate the natural ventilation performance of the prototype building.
CFD modelling of naturally ventilated double-skin facades with Venetian blinds [111]	2008	Naturally ventilated DSF with integrated venetian blinds	Different slat angles	Ansys CFX10	Finite volume (2D)	k-ω model	Hybrid mesh (rectangles + triangles)	By own experiment: thermal part: yes, dynamical part: incomplete.	Fully implicit	Multi-band Monte Carlo model	Numerical study on naturally ventilated DSF that inspects influence of venetian blinds on the flow and heat transfer in the cavity.
Nodal network and CFD simulation of airflow and heat transfer in double skin facades with blinds [112]	2008	Naturally ventilated DSF with integrated venetian blinds	Numerical approaches comparison.	Ansys CFX5.7.1	Finite volume (3D)	k-ω model	Not specified	By own experiment: thermal part: yes, dynamical part: incomplete.	Not specified	Multi-band Monte Carlo model	A simplified and CFD model was developed in order to compare their performance in the prediction of heat transfer and buoyancy-driven airflow. First developed three-dimensional CFD model of naturally ventilated DSF with integrated venetian blinds.
Numerical investigation on thermal	2008	Naturally ventilated DSF with	Different cavity depth, aspect ratio, height,	Phoenics 3.6	Finite volume (3D)	RNG k- ε model	Structured mesh (rectangles)	By open literature experimental	Not specified	Not specified	Based on the CFD simulation results,

(continued on next page)

Table A.2 (*continued*)

Name	Year	Examined configuration	Examined constructional features/ quantities	Used tool	Discretization method and dimensionality	Turbulence model	Grid type	Validation	Solution algorithm	Radiation model	The description
performance and correlations of double skin facade with buoyancy-driven airflow [44]		integrated roller blind	opening size, type of shading and environmental conditions					database [84]: thermal part: yes, dynamical part: incomplete			correlations for cavity airflow rate, air temperature stratification, and interior convection coefficient were provided.
Natural ventilation in the double skin facade with venetian blind [33]	2008	Naturally ventilated DSF with integrated venetian blinds	Shading position (fixed angle 45^0 and position: middle).	Not specified	Finite volume	Not specified	Not specified	By open literature experimental database [76]: thermal part: yes, dynamical part: no	Not specified	Separate model	In the paper, a detailed analysis of the thermal process in DSF with venetian blind was made. The governing equations were solved by incorporating CFD, optical and heat balance model. There is a lack of information on the CFD model.
Double skin façades for warm climate regions: Analysis of a solution with an integrated movable shading system [74]	2009	Naturally and mechanically ventilated DSF with integrated blinds.	Winter configuration: closed natural, O–O natural and forced O–I ventilation mode. Summer configuration with closed blinds.	Ansys Fluent 6.2	Finite volume (2D/3D)	RNG k-ε model	Unstructured mesh (triangles for 2D and tetrahedral for 3D)	By open literature experimental database [127]: thermal part: yes, dynamical part: incomplete.	Not specified	The solar ray tracing model	CFD model has been built and in order to compare the energy performance of one summer and three winter configurations with the energy performance of traditional enclosures.
A CFD approach to evaluate the influence of construction and operation parameters on the performance of active transparent facades in Mediterranean climates [80]	2009	Mechanically ventilated DSF	Different Reynolds number, length-to-depth ratio, glazing emissivity and transmittivity and inlet configuration.	Ansys Fluent 6.3	Finite volume (3D)	RNG k-ε model	Structured mesh (rectangular cuboids)	CFD model has been validated in previous works [120] by experimental database [76]. No further information.	PISO	P1 radiation model	This study assess, using CFD as a tool, the influence of optical properties of the materials, geometrical relations of the façade and flow stream conditions on energy savings, measured through reduction of the solar heat gain.
Numerical evaluation of the mixed convective heat transfer in a double-pane window integrated with see-through a-Si PV cells with low-e coatings [31]	2010	Naturally ventilated DSF	Different Rayleigh numbers and effects of low-e coatings applied on glazing.	Own numerical code (Fortran 90)	Finite difference (2D)	No turbulence model (laminar)	Not specified	Not validated	successive under-relaxation method (SUR)	Radiosity equation	2D numerical analysis of the control strategies on potential energy savings in double-pane window integrated with transparent a-S photovoltaic with low emittance (low-e) coatings.
CFD Analysis of Turbulent Natural Ventilation in Double-Skin	2010	Naturally ventilated DSF with integrated	Cross-comparison of different DSF types: no	Ansys Fluent 6.3	Finite volume (2D)	Standard k-ε model	Hybrid mesh (rectangles + triangles)	By open literature experimental database [75]:	Not specified	The discrete ordinates	This work summarizes the results of a computational

(continued on next page)

Table A.2 (*continued*)

Name	Year	Examined configuration	Examined constructional features/ quantities	Used tool	Discretization method and dimensionality	Turbulence model	Grid type	Validation	Solution algorithm	Radiation model	The description
Facade: Thermal Mass and Energy Efficiency [110]		venetian blinds	blinds, with aluminum blinds and with thermal mass concrete.					thermal part: no, dynamical part: incomplete.		(DO) model	fluid dynamic (CFD) analysis, which was carried out to investigate the effect of blind and thermal mass concrete on the thermal performance of a double-skin façade.
Natural Convection in PV-Integrated Double-Skin Façade using Large-Eddy simulation [37]	2011	Vertical parallel plates channel naturally ventilated	Cavity	Own numeric code	Finite volume (3D)	No. Large Eddy Simulation (Vreman subgrid-scale model)	Not specified	By open literature experimental database [86]: thermal part: yes, dynamical part: fully.	Two-stage predictor corrector method	Not included	First LES simulation on DSF. Useful observations on the advantages of LES over RANS in modeling naturally induced turbulent flow have been made.
Airflow and heat transfer in double skin facades [78]	2011	Mechanically ventilated DSF with integrated venetian blinds	Different slat angles and position of the blinds	Ansys Fluent 6.3	Finite volume (2D)	RNG k-ε model	Not specified	By own experiment: thermal part: yes, dynamical part: no	SIMPLE	The S2S (surface to surface) radiation model	CFD model has been developed for mechanically ventilated DSF with integrated venetian blinds in order to asses thermal and fluid dynamics behavior of DSF in response to position and angle of venetian blinds.
Numerical simulation of dynamical aspects of natural convection flow in a double-skin façade [41]	2012	Vertical parallel plates channel naturally ventilated (filled with water)	Different Rayleigh numbers and aspect ratios	Ansys Fluent (version not specified)	Finite volume (2D)	No turbulence model (laminar).	Structured mesh (rectangles)	By own experiment: thermal part: no dynamical part: incomplete	Not specified	Not included	A 2D numerical study of the laminar flow in an asymmetrically heated vertical plane channel with variable different Rayleigh numbers and aspect ratios. Water as a working medium.
Evaluation of various CFD modelling strategies in predicting airflow and temperature in a naturally ventilated double skin façade [6]	2012	Naturally ventilated DSF	Numerical approaches comparison	Ansys Fluent 6.3	Finite volume (2D/3D)	SST k-ω and RNG k-ε model.	Not specified	By open literature experimental database [47]: thermal part: yes, dynamical part: fully.	SIMPLE	Not included (measured values used)	A useful numerical study that highlights which segments of the CFD model are important in the simulation of thermo-physical behavior of naturally ventilated DSF. Dimensionality, turbulence models, modelization of external environment and fluid

(*continued on next page*)

Table A.2 (*continued*)

Name	Year	Examined configuration	Examined constructional features/ quantities	Used tool	Discretization method and dimensionality	Turbulence model	Grid type	Validation	Solution algorithm	Radiation model	The description
											properties are subjected to a sensitivity analysis, upon which a conclusion about the preferred CFD strategy has been drawn.
An experimentally validated mathematical and CFD model of a supply air window: Forced and natural flow [54]	2013	Naturally and mechanically ventilated DSF	Mechanically ventilated DSF with two different airflow rates and one naturally ventilated DSF.	Ansys Fluent 12.1	Finite volume (3D)	SST k–ω model	Structured mesh (rectangular cuboids)	By own experiment: thermal part: yes, dynamical part: incomplete	SIMPLE	The solar ray tracing model	CFD 3D model has been used for modelling airflow in DSF with supply ventilation mode for both types of DSF (naturally and mechanically ventilated) without venetian blinds.
Analysis of ventilation effects and the thermal behavior of multifunctional facade elements with 3D CFD models [123]	2014	Three different naturally ventilated DSFs: with integrated photovoltaic module (PV), a solar collector (ST) and a classic DSF design with two transparent glazing.	Cross comparison of three DSF types in typical summer conditions (25 °C, 500 Wm^{-2} and 60° incident angle)	Ansys Fluent 14.0	Finite volume (3D)	RNG k- ε model	Structured mesh (rectangular cuboids)	By own experiment: thermal part: yes, dynamical part: incomplete	SIMPLE	The discrete ordinates (DO) model	This study determines thermal behavior and airflow characteristics of three types of naturally ventilated DSFs using CFD simulations.
Double Skin Façade: Modelling Technique and Influence of Venetian Blinds on the Airflow and Heat Transfer [113]	2014	Naturally ventilated DSF with integrated venetian blinds	Different blind angles and position of the shading system.	Ansys Fluent 14.0	Finite volume (3D)	RNG k- ε model	Hybrid (tetrahedral and rectangular cuboids)	By open literature numerical database [47]: thermal part: yes, dynamical part: no.	SIMPLE	The solar ray tracing model/The discrete ordinates (DO) model	In this paper four modelling strategies and the influence of blind tilt angle and their proximity to the façade walls are investigated through 3D CFD simulations.
Thermal Performance of Ventilated Double Skin Façades with Venetian Blinds [12]	2015	Mechanically ventilated DSF with integrated venetian blinds	Different emissivity and absorptivity of blinds, shading position and airflow rate.	Ansys Fluent 15.0	Finite volume (3D)	RNG k-ε model	Structured mesh (rectangular cuboids)	By open literature experimental database [76]: thermal part: yes, dynamical part: fully.	PISO	P1 radiation model	The influence of several optical and geometrical properties of blinds and ventilation rate conditions of a DSF on the reduction of solar heat gains has been evaluated in this CFD study.
A numerical analysis of the air ventilation management and assessment of the behavior of double skin facades [58]	2015	Mechanical DSF with integrated venetian blinds	Different slat angles, incident angle of solar radiation, the slat emissivity and the airflow rate.	Ansys Fluent 6.3	Finite volume (2D)	Realizable k–ε model	Unstructured (triangles)	By open literature experimental database [53]: thermal part: no, dynamical part: fully.	SIMPLE	The discrete ordinates (DO) model	This research through developed CFD model examines the effect of solar radiation, incidence angle and slat angle on the thermal properties and the solar transmission

(*continued on next page*)

Table A.2 (*continued*)

Name	Year	Examined configuration	Examined constructional features/ quantities	Used tool	Discretization method and dimensionality	Turbulence model	Grid type	Validation	Solution algorithm	Radiation model	The description
											into the interior environment for a DSF equipped with a venetian blind.
Modelling natural ventilation in double skin façade [102]	2015	Naturally ventilated DSF	Numerical approaches comparison	OpenFOAM	Finite volume (2D)	The q-ζ model/RNG k-ε model	Structured (rectangles)	By open literature experimental database [48]: thermal part: yes, Dynamical part: incomplete.	SIMPLE	Not included (measured values used)	The CFD modelling activity presented in this work aims at investigating the reliability of the assumptions and hypotheses employed in the simplified model.
Solar heat gain reduction of double-glazing window with cooling pipes embedded in venetian blinds by utilizing natural cooling [118]	2016	Naturally ventilated DSF with integrated cooling pipes embedded in the venetian blinds	Cross-comparison of three types of DSF: no blinds, with blinds and with blinds accompanied with cooling pipes. Influence of glazing type.	Ansys Fluent 14.5	Finite volume (2D)	RNG k-ε model	Hybrid (rectangles and triangles)	By open literature experimental database [122]: thermal part: yes dynamical part: incomplete	SIMPLE	The Discrete Ordinate Method (DOM)	Cooling pipes embedded in the venetian blinds of a DSF are presented in this study along with a CFD model for the analysis of the effect of embedded pipes, different structures and glass assemblies on the thermal behavior of DSF.
Thermal performance of double skin façade with built-in pipes utilizing evaporative cooling water in cooling season [119]	2016	Naturally ventilated DSF with integrated cooling pipes embedded in the venetian blinds	Six different DSF configuration with open/ closed vents and Y/N built-in pipes. Different climate and orientation of DSF.	ANSYS Fluent 14.5	Finite volume (2D)	Standard k-ε model	Hybrid (rectangles and triangles)	By open literature experimental database [122]: thermal part: yes dynamical part: incomplete	SIMPLE	The Discrete Ordinate Method (DOM)	A comprehensive numerical model is presented to simulate the dynamic heat transfer during the cooling season where the performance of the pipe embedded DSF is investigated regarding different ventilation and operation strategies. The heat transfer process of the novel DSF is analyzed and compared with the traditional DSF. And influencing factors such as climate and orientation are evaluated.
Experimental and numerical investigation of natural convection in a double skin façade [42]	2016	Naturally ventilated DSF	Different Rayleigh numbers.	Ansys Fluent 14.5	Finite volume (3D)	Realizable k-ε model	Structured mesh (rectangular cuboids)	By own experiment: thermal part: yes. By open literature experimental database [52]: dynamical part: fully.	SIMPLE	Not included (measured values used)	Based upon the developed CFD model, the correlation for Nusselt number as a function of a Rayleigh number are given.

(*continued on next page*)

Table A.2 (*continued*)

Name	Year	Examined configuration	Examined constructional features/ quantities	Used tool	Discretization method and dimensionality	Turbulence model	Grid type	Validation	Solution algorithm	Radiation model	The description
Numerical and experimental investigation of unsteady natural convection in a non-uniformly heated vertical open-ended channel [38]	2016	Vertical parallel plates channel naturally ventilated	Uniformly and non-uniformly heated side of cavity.	Own numeric code	Finite volume (3D)	No. Large Eddy Simulation (Vreman subgrid-scale model)	Structured mesh (rectangular cuboids)	By own experiment: thermal part: yes, dynamical part: fully.	Two-step predictor corrector method	The radiosity model	LE simulation that includes the radiosity model describes characteristics of the flow behavior in and gives a preferred arrangement of PV panels in order to avoid overheating in the cavity.
Effect of Emissivity of Shading Device and Air Flow Inside Cavity of Double Skin Facade for Energy Saving and Thermal Comfort in Buildings: A CFD Modeling [115]	2016	Naturally ventilated DSF with integrated venetian blinds	Different airflow rate and emissivity of shading device.	Ansys Fluent 14.0	Finite volume (2D)	RNG k-ε model	Unstructured (triangles)	CFD model has been fully validated in previous works [113] by experimental measurements [47].	Not specified	The Discrete Ordinate Method (DOM)	The influence of different airflow rates and emissivity of the shading device is analyzed through the CFD model.
Influence of natural ventilation due to buoyancy and heat transfer in the energy efficiency of a double skin facade building [96]	2016	Naturally ventilated DSF	Different cavity widths in winter/ summer conditions with opened/closed vents and with/ without solar radiation.	Ansys Fluent 14.0	Finite volume (2D)	RNG k–ε model	Structured (rectangles)	By open literature numerical database [128]; [129] (not specified how).	SIMPLE	Separate model	A simplified model was simulated using CFD software to investigate the effects due to different cavity widths in winter and summer conditions with opened and closed vents and considering solar radiation or not.
Effect of inclination angle of the adiabatic wall in asymmetrically heated channel on natural convection: Application to double-skin façade design [95]	2017	Vertical parallel plate channel naturally ventilated with possibility of side inclination	Different inclination angles of walls.	Ansys Fluent (version not specified)	Finite volume (2D)	No turbulence model	Structured mesh (rectangles)	By open literature experimental database [41]: thermal part: yes, dynamical part: fully.	–	Not included	Numerical study about natural laminar flow in the cavity and the influence of different inclination of sides and UHF conditions on heat and mass flow rate has been investigated.
Experimental and Numerical Investigation of Forced Convection in a Double Skin Façade [43]	2017	Mechanically ventilated DSF	Different aspect ratio and airflow rate.	Ansys Fluent 16.0	Finite volume (3D)	Realizable k-ε model	Structured mesh (rectangular cuboids)	By own experiment: thermal part: yes, dynamical part: fully.	SIMPLE	Not included	Based upon the developed CFD model, the correlation for Nusselt number is given as a function of an aspect ratio and Reynolds number. Interesting findings on thermal and hydrodynamic entrance length of mechanically induced flow are given. Flow features and geometrical characteristics of DSF that can increase fan

(*continued on next page*)

Table A.2 (*continued*)

Name	Year	Examined configuration	Examined constructional features/ quantities	Used tool	Discretization method and dimensionality	Turbulence model	Grid type	Validation	Solution algorithm	Radiation model	The description
											consumption are highlighted.
Naturally ventilated double-skin facade in modeling and experiments [90]	2017	Naturally ventilated DSF with integrated venetian blinds	Four situations where flow is differently driven by buoyancy and wind.	Open FOAM	Finite volume (2D)	SST k-ω model	Structured mesh (rectangles)	By own experiment: thermal part: yes, dynamical part: fully.	PISO	Not included (measured values used)	A simplified and CFD model has been developed in order to compare their performance in modelling mass flow rate and temperature distribution of naturally ventilated DSF. One of the rare CFD studies that analyses the influence of both wind and buoyancy on the temperature and velocity profile inside the cavity.
Design of a glazed double-façade by means of coupled CFD and building performance simulation [85]	2017	Naturally ventilated DSF	Thermal behavior of multi-storey DSF façade during summer weather.	StarCCM+	Finite volume (3D)	Standard k-ε model	Unstructured (not specified)	Not validated	Not specified	Not specified	In this paper, 3D CFD model is coupled with the BPS tool (IDA-ICE) in order to investigate the warm day cycle and its effects on the interiors.
Heat transfer analysis of an integrated double skin façade and phase change material blind system [64]	2017	Naturally ventilated DSF with integrated PCM blind system	Cross-comparison of DSF with PCM and aluminum blinds.	Ansys Fluent 14.0	Finite volume (2D)	RNG k-ε model	Hybrid mesh (rectangles + triangles)	By own experiment: thermal part: yes, dynamical part: no.	SIMPLE	The discrete ordinates (DO) model	CFD model that considers heat transfer on/ through PCM blinds has been developed. The influence of PCM blinds on the removal of excessive heat and stabilization of the flow in the cavity has been investigated.
Numerical investigation into a double skin façade system integrated with shading devices, with reference to the city of Amman, Jordan [98]	2017	Naturally ventilated DSF with integrated venetian blinds	Size, inclination angle, position, surface emissivity and surface diffuse fraction of slats and surface diffuse fraction of glass panes.	Ansys Fluent (version not specified)	Finite volume (2D)	RNG k-ε and SST k – ω model	Hybrid mesh (rectangles + triangles)	By open literature experimental database [47]: thermal part: yes, dynamical part: fully.	SIMPLE	The discrete ordinates (DO) model	The doctoral thesis includes parametric study concerning configuration and design parameters of both DSF's cavity and shading slats, in addition to boundary conditions. For the purpose of this study, a CFD-Fluent model was developed and validated.
Potential application of double skin façade incorporating aerodynamic modifications for wind energy harvesting [104]	2018	Naturally ventilated DSF	Different wind directions, different opening arrangements (recessed regions, curved walls)	ANSYS Fluent 13.0	Finite volume (3D)	SST k-ω model	Structured (rectangular cuboids)	By own experiment [106]	The pressure-based solver (not specified)	–	Experimentally validated CFD study that investigates a method for wind energy harvesting and the effect of

(*continued on next page*)

Table A.2 (*continued*)

Name	Year	Examined configuration	Examined constructional features/ quantities	Used tool	Discretization method and dimensionality	Turbulence model	Grid type	Validation	Solution algorithm	Radiation model	The description
											aerodynamic modifications: recessed regions and curved walls, on the flow characteristics inside an empty corridor-type DSF on high-rise building. Only wind as a driving force is examined.
Performance assessment of a special Double Skin Façade system for wind energy harvesting and a case study [91]	2018	Naturally ventilated DSF	Different wind intensity and incident angle.	ANSYS Fluent 13.0	Finite volume (3D)	SST k-ω model	Structured (rectangular cuboids)	By own experiment [106]	The pressure-based solver (not specified)	–	Experimentally validated CFD simulations were performed to assess the wind energy potential of corridor-type DSF placed on high-rise buildings.
Solar Heat Gain Coefficient Analysis of a Slim-Type Double Skin Window System: Using an Experimental and a Simulation Method [68]	2018	Naturally ventilated DSF (slim-type) equipped with venetian blinds	Different openings (different ventilation modes).	Star CCM+	Finite volume (3D)	Realizable k-ε model	Structured (rectangular cuboids)	By own experiment: Solar heat coefficient validated thermal part: no, dynamical part: no,	SIMPLE	The S2S (surface to surface) radiation model	Solar heat gain coefficients and the cavity temperatures are experimentally measured in order to analyze the opening influence on cooling energy needs of a special type of double skin facades (slim-type) of double skin window system with 270 mm wide cavity).
Experimental and numerical analysis of a naturally ventilated double-skin façade [60]	2018	Natural opaque DSF	Cross-comparison with standard opaque (one-skin) wall.	Ansys CFX	Finite volume (3D)	Standard k-ε model	Structured (rectangular cuboids)	By own experiment: Thermal part: yes, Dynamical part: no.	Not specified	Monte Carlo model	CFD analysis on the thermal behavior of the natural opaque DSF and its comparison with thermal behavior of standard one-skin wall.
Phase change material blind system for double skin façade integration: System development and thermal performance evaluation [65]	2019	Naturally ventilated DSF with integrated PCM blind system	Different PCM blind angles and position of shading system. Comparison with aluminum blinds.	Ansys Fluent (version not specified)	Finite volume (2D)	RNG k-ε model	Hybrid mesh (rectangles + triangles)	By own experiment: thermal part: yes, dynamical part: no.	SIMPLE	The discrete ordinates (DO) model	One of the papers in series that analyses thermal behavior of DSF with integrated PCM blinds with CFD model that is validated using a natural experiment in The Centre for Sustainable Energy Technologies (Nottingham, China).
Effective use of venetian blind in Trombe wall for	2019	Trombe wall naturally ventilated	Different incident solar radiation,	Ansys Fluent 6.3	Finite volume (2D)	k-ω turbulence model	Structured (rectangles)	By own experiment: thermal part:	SIMPLE	The S2S (surface to surface)	In this study, the thermal performance of

(continued on next page)

Table A.2 (*continued*)

Name	Year	Examined configuration	Examined constructional features/ quantities	Used tool	Discretization method and dimensionality	Turbulence model	Grid type	Validation	Solution algorithm	Radiation model	The description
solar space conditioning control [71]		with integrated venetian blinds	distance between blinds, slat angle, inlet width and outlet vent width for two modes: cooling and natural ventilation mode.					yes dynamical part: incomplete		radiation model	the Trombe wall with venetian blind in the cooling season was analyzed by coupling Computational Fluid Dynamics (CFD) modelling and Building Energy Simulation (BES).
Effects of radiation on turbulent natural convection in channel flows [130]	2019	Vertical parallel plate channel naturally ventilated	Different values of emissivity of the channel walls, and different relative humidity of the ambient air.	Own numerical code (Fortran)	Finite volume (3D)	No. Large Eddy Simulation (Vreman subgrid-scale model)	Structured (refinement)	Not validated	PCGS (preconditioned conjugate-gradient) solver	The discrete ordinate (DO) model	A computational study using the LES approach has been undertaken where a constant heat flux of 220 W/m^2 is imposed on one side of the vertical parallel channel in order to analyze the complex interaction of radiation with the natural flow of dry and humid air.
Investigation on thermal performance of an integrated phase change material blind system for double skin facade buildings [116]	2019	Naturally ventilated DSF with integrated PCM blinds	Cross-comparison of DSF with PCM and aluminum blinds.	Ansys Fluent (version not specified)	Finite volume (not specified)	RNG k-ε model	Not specified	By own experiment (not specified how)	SIMPLE	The discrete ordinate (DO) model	One of the papers in series that analyses thermal behavior of DSF with integrated PCM blinds and compares with conventional DSF with aluminum blinds during the hot summer period. The paper does not contain enough information about the numerical model, but it is supposed that the same model is used as in previous works of Li and Darkwa.
Effect of design parameters on thermal performance of integrated phase change material blind system for double skin façade buildings [117]	2019	Naturally ventilated DSF with integrated PCM blinds	Different angle of PCM blinds, position of PCM shading system and type of blinds (aluminum and two types of PCM)	Ansys Fluent 14.5	Finite volume (not specified)	RNG k-ϵ model	Not specified	By own experiment: thermal part: yes dynamical part: no	SIMPLE	The discrete ordinate (DO) model	This paper focuses on the effect of design parameters on the thermal performance of such systems by conducting a simulation study of a DSF integrated with a PCM blind with different material properties,

(*continued on next page*)

Table A.2 (*continued*)

Name	Year	Examined configuration	Examined constructional features/ quantities	Used tool	Discretization method and dimensionality	Turbulence model	Grid type	Validation	Solution algorithm	Radiation model	The description
											positions in the cavity, and tilt angles of blades.
Cooling energy performance and thermal characteristics of a naturally ventilated slim double-skin window [40]	2019	Naturally ventilated DSF (slim-type)	Three types of different outer glazing: clear, colored and low-e glass.	Star CCM+	Finite volume (3D)	RNG k-ϵ model	Not specified	By own experiment: thermal part: yes dynamical part: no	SIMPLE	The S2S (surface to surface) radiation model and multiband thermal radiation model	This study aims to analyze the cooling energy performance of slim-type DSF through the numerical study that investigates the influence of outer single glazing on it.
Thermal and energy performance investigation of a smart double skin facade integrating vanadium dioxide through CFD simulations [72]	2019	Naturally ventilated DSF with opaque inner side (with AlN coating)	Different air gap thicknesses.	Ansys Fluent 15.0	Finite volume (2D)	No. Unsteady Reynolds Averaged Navier Stockes equations (URANS equations)	Structured (rectangles)	By open literature experimental database [131]: thermal part: yes, dynamical part: no.	Not specified	The S2S (surface to surface) radiation model	The aim of simulations are to investigate the thermal performance of a DSF that integrates Tungsten (W) doped Vanadium dioxide (VO2) as an optically smart material on outer glazing and a high absorbing aluminum nitride (AlN) coating on the inner facade. A parametric study was carried out in order to analyze the impact of the air cavity thickness on the thermal behavior.
Flow and heat transfer characteristics of natural convection in vertical air channels of double-skin solar façades [92]	2019	Naturally ventilated DSF with integrated PV module absorber on inner opaque side	Different channel widths and heights and input heat fluxes.	Ansys Fluent 6.3	Finite volume (3D)	Standard k-ε model	Structured (rectangular cuboids)	By open literature experimental database [132]: thermal part: yes dynamical part: yes	SIMPLE	Separate model	This study numerically investigates the flow and heat transfer process in the vertical parallel plate channel under influence of different widths and heights of the channel and imposing heat fluxes.
Simulation of the thermal performance of a geometrically complex Double-Skin Facade for hot climates: EnergyPlus vs. OpenFOAM [94]	2019	Naturally ventilated DSF	Numerical approaches comparison.	OpenFOAM	Finite volume (3D)	Standard k-ε model	Not specified	Not validated	SIMPLE	Not included (boundary conditions taken from Energy Plus)	A numerical experiment is performed in which two models of a DSF are compared; one simulated with EnergyPlus and the other with OpenFOAM CFD software. Using CFD, the aims is to better understand the thermal performance of the DSF.

(*continued on next page*)

Table A.2 (*continued*)

Name	Year	Examined configuration	Examined constructional features/ quantities	Used tool	Discretization method and dimensionality	Turbulence model	Grid type	Validation	Solution algorithm	Radiation model	The description
Experimental Validation of a Numerical Model of a Ventilated Façade with Horizontal and Vertical Open Joints [108]	2019	Naturally ventilated DSF	Opening arrangement (ventilation mode). Validation of numerical model.	Ansys Fluent (version not specified)	Finite volume (3D)	RNG k-ε turbulence model	Hybrid (tetrahedral and rectangular cuboids)	Validated with own experiment: thermal part: yes, dynamical part: full.	SIMPLE	The discrete ordinate (DO) model	This paper experimentally validates a numerical simulation model of a Ventilated Façade with Horizontal and Vertical Open Joints (OJVF).
Experimental and numerical natural convection in an asymmetrically heated double vertical façade [87]	2020	Vertical parallel plates naturally ventilated	Two cases (the constant heat flux and the constant temperature): different Rayleigh numbers and aspect ratios.	Ansys Fluent (version not specified)	Finite volume (2D)	No turbulence model (laminar).	Structured (rectangles)	By open literature experimental database [133] and by own experiment: thermal part: yes, dynamical part: no.	SIMPLE	The discrete ordinate (DO) model/No radiation model	Study on laminar flow in an asymmetrically heated open double vertical façade naturally ventilated. Turbulent quantity analysis can be useful for DSF under certain conditions.
Application of double-glazed façades with horizontal and vertical louvers to increase natural air flow in office buildings [109]	2020	Naturally ventilated DSF with integrated horizontal and vertical louvers	Two types of naturally ventilated DSFs with integrated horizontal and vertical louvers.	Ansys Fluent (version not specified)	Finite volume (2D)	RNG k-ε model	Hybrid (rectangles + triangles)	By open literature experimental database [47]: thermal part: yes, dynamical part: fully.	SIMPLE	The discrete ordinate (DO) model	Numerical simulation of airflow and heat transfer inside the cavity of the DSF and the effect of different types of solar shading systems in horizontal and vertical modes on the airflow has been investigated using the CFD technique.
Natural ventilation of double skin façade: Evaluation of wind-induced airflow in tall buildings [105]	2020	Naturally ventilated DSF (wind only)	Different wind directions and speeds at three building levels: bottom, middle and top.	Ansys Fluent 19.0	Finite volume (3D)	SST k–ω model	Structured (rectangular cuboids)	CFD validated in previous researches [106].	SIMPLE	–	A series of CFD simulations were conducted on two basic wind-induced DSF configurations considering four wind incident angles (0°, 30°, 60°, and 90°).
Simulation and experimental verification of energy saving effect of passive preheating natural ventilation double skin façade [93]	2020	Naturally ventilated DSF	Different height, position of opening, winter scenarios and orientations.	Not specified	Finite volume (3D)	Standard k-ε model	Not specified	By own experiment: thermal part: yes, dynamical part: no.	Not specified	Not specified	This paper analyzes the passive preheating and the influence of the structural parameters of the double skin facade in cold season ventilation on the preheating ventilation effect. Important information on the CFD model is missing in research.
Computational fluid dynamics assessment for the thermal	2020	Naturally ventilated DSF with integrated	Different cavity depth, opening size and louver blinds ON/OFF	Star CCM+	Finite volume (3D)	RNG k–e turbulence model	Not specified	By open literature experimental database [47]	SIMPLE	Not specified	The impact of various configurations on the thermal

(*continued on next page*)

Table A.2 (*continued*)

Name	Year	Examined configuration	Examined constructional features/ quantities	Used tool	Discretization method and dimensionality	Turbulence model	Grid type	Validation	Solution algorithm	Radiation model	The description
performance of double-skin facades in office buildings under hot climatic condition [99]		venetian blinds						(not specified how).			performance of the DSF is evaluated under the weather situation (summer) in Saudi Arabia through CFD simulations.
Ventilation performance of a naturally ventilated double-skin façade in buildings [100]	2020	Naturally ventilated DSF	Cavity depth, size of openings, glazing area, ventilation mode, DSF location and room dimensions.	Ansys Fluent 2020R1	Finite volume (3D)	RNG k-ε model	Structured (rectangular cuboids)	By open literature experimental database[126]: thermal part: yes, dynamical part: no.	COUPLED	The discrete ordinates (DO) model	The impact of cavity depth, size of openings, glazing area, ventilation mode, DSF location and room dimensions on naturally induced flow was evaluated in this experimentally validated CFD research.

References

[1] E. Oesterle, R.-D. Lieb, M. Lutz, W. Heusler, Double-skin Facades : Integrated Planning, München : Prestel, 2001.
[2] S. Barbosa, K. Ip, Perspectives of double skin façades for naturally ventilated buildings: a review, Renew. Sustain. Energy Rev. 40 (2014) 1019–1029.
[3] M.M.S. Ahmed, A.K. Abel-Rahman, A.H.H. Ali, M. Suzuki, Double skin façade: the state of art on building energy efficiency, J. Clean Energy Technol. 4 (1) (2015) 84–89.
[4] C. Hachem-Vermette, in: " C. Hachem-Vermette (Ed.), Selected High-Performance Building Envelopes BT - Solar Buildings and Neighborhoods: Design Considerations for High Energy Performance, Springer International Publishing, Cham, 2020, pp. 67–100.
[5] M.a. Shameri, M.a. Alghoul, K. Sopian, M.F.M. Zain, O. Elayeb, Perspectives of double skin façade systems in buildings and energy saving, Renew. Sustain. Energy Rev. 15 (3) (Apr. 2011) 1468–1475.
[6] W. Pasut, M. De Carli, Evaluation of various CFD modelling strategies in predicting airflow and temperature in a naturally ventilated double skin façade, Appl. Therm. Eng. 37 (2012) 267–274.
[7] M.H. Oh, K.H. Lee, J.H. Yoon, Automated control strategies of inside slat-type blind considering visual comfort and building energy performance, Energy Build. 55 (Dec. 2012) 728–737.
[8] M.G. Gomes, A.J. Santos, A.M. Rodrigues, Solar and visible optical properties of glazing systems with Venetian blinds: numerical, experimental and blind control study, Build. Environ. 71 (2014) 47–59. Complete.
[9] M. Al Kaabi, Double Skin Façade as an Urban Heat Island Mitigation Strategy-Case Study of a Health Care Facility in Abu Dhabi, Masdar Institute of Science and Technology, 2016.
[10] H. Andoni, S. Wonorahardjo, A review on mitigation technologies for controlling urban heat island effect in housing and settlement areas, IOP Conf. Ser. Earth Environ. Sci. 152 (May 2018), 012027.
[11] A.H. Block, S.J. Livesley, N.S.G. Williams, Responding to the urban heat island: a review of the potential of green infrastructure, Vic. Cent. forClimate Chang. Adapt. Res. Melb. (2012).
[12] J. Parra, A. Guardo, E. Egusquiza, P. Alavedra, Thermal performance of ventilated double skin façades with Venetian blinds, Energies 8 (6) (2015) 4882–4898.
[13] D. Faggembauu, Heat Transfer and Fluid-Dynamics in Double and Single Skin Facades, " Universitat Politècnica de Catalunya, 2006.
[14] H. Hens, Building Physics - Heat, Air and Moisture: Fundamentals and Engineering Methods with Examples and Exercises, 2012.
[15] J.H. Ferziger, M. Perić, Computational Methods for Fluid Dynamics, 1996.
[16] V. Gavan, M. Woloszyn, F. Kuznik, J.-J. Roux, Experimental study of a mechanically ventilated double-skin façade with Venetian sun-shading device: a full-scale investigation in controlled environment, Sol. Energy 84 (2) (2010) 183–195.
[17] M. Dopudi, "Naturally Ventilated Double Skin Facade : CFD and Simplified Model for Parametric Energy Simulation, Politecnico Milano, 2017.
[18] A. De Gracia, A. Castell, L. Navarro, E. Oró, L.F. Cabeza, Numerical modelling of ventilated facades: a review, Renew. Sustain. Energy Rev. 22 (2013) 539–549.
[19] J. Zhou, Y. Chen, A review on applying ventilated double-skin facade to buildings in hot-summer and cold-winter zone in China, Renew. Sustain. Energy Rev. 14 (4) (2010) 1321–1328.
[20] G. Cattarin, et al., Empirical validation and local sensitivity analysis of a lumped-parameter thermal model of an outdoor test cell, *Build. Environ.*, Feb. (2018).
[21] E. Catto Lucchino, F. Goia, G. Lobaccaro, G. Chaudhary, Modelling of double skin facades in whole-building energy simulation tools: a review of current practices and possibilities for future developments, Build. Simul. 12 (1) (2019) 3–27.
[22] S.S.M. Foroushani, A New Technique for Characterizing Multi-Temperature Convection with Application in Building Energy Simulation, University of Waterloo, 2017.
[23] S. Foroushani, D. Naylor, J. Wright, A new formulation for convection problems entailing multiple isothermal boundaries, Int. J. Therm. Sci. 129 (2018) 396–403.
[24] S. Foroushani, D. Naylor, J.L. Wright, Heat transfer correlations for laminar free convection in vertical channels with asymmetrically heated isothermal walls, Heat Tran. Eng. 41 (5) (2020) 418–432.
[25] S. Foroushani, J.L. Wright, D. Naylor, Turbulent free convection in a vertical channel with isothermal walls: new formulation and the resistor-network model, Comput. Therm. Sci. 11 (1–2) (2019) 131–145.
[26] S.S.M. Foroushani, J.L. Wright, D. Naylor, Asymmetric graetz problem: the analytical solution revisited, J. Thermophys. Heat Tran. 31 (1) (2017) 237–242.
[27] S.S.M. Foroushani, D. Naylor, J.L. Wright, Convective heat transfer in hydrodynamically developed laminar flow in asymmetrically heated annuli: a three-temperature problem, in: Proceedings of the 12th Intl. Conf. Heat transfer Fluid Mechanics & Thermodynamics (HEFAT2016), 2016, pp. 527–532.
[28] S. Foroushani, J.L. Wright, D. Naylor, Resistor-network formulation of multitemperature free-convection problems, J. Thermophys. Heat Tran. 31 (3) (2017) 628–633.
[29] S.S.M. Foroushani, D. Naylor, J.L. Wright, "Convective heat transfer in hydrodynamically - developed laminar flow in asymmetrically - heated Annuli : a three-temperature problem, in: Proceedings of the 12th Intl. Conf. Heat Transfer Fluid Mechanics & Thermodynamics (HEFAT2016), 2016, pp. 527–532.
[30] J.L.M. Hensen, R. Lamberts, Building Performance Simulation for Design and Operation, vol. 9780203891, 2012.
[31] J. Han, L. Lu, H. Yang, Numerical evaluation of the mixed convective heat transfer in a double-pane window integrated with see-through a-Si PV cells with low-e coatings, Appl. Energy 87 (11) (2010) 3431–3437.
[32] S. Tkachenko, V. Timchenko, G. Yeoh, J. Reizes, Effects of radiation on turbulent natural convection in channel flows, Int. J. Heat Fluid Flow 77 (2019) 122–133.
[33] X. li Xu, Z. Yang, Natural ventilation in the double skin facade with Venetian blind, Energy Build. 40 (8) (2008) 1498–1504.
[34] Z.J. Zhai, Z. Zhang, W. Zhang, Q.Y. Chen, "Evaluation of various turbulence models in predicting airflow and turbulence in enclosed environments by cfd: Part 1—summary of prevalent turbulence models, HVAC R Res. 13 (6) (2007) 853–870.

[35] J. Smagorinsky, General circulation experiments with the primitive equations: 1. The basic experiment, Mon. Weather Rev. (1963).
[36] J.W. Deardorff, A numerical study of three-dimensional turbulent channel flow at large Reynolds numbers, J. Fluid Mech. 41 (2) (1970) 453–480.
[37] G.E. Lau, G.H. Yeoh, V. Timchenko, R.K.K. Yuen, Natural convection in a PV-integrated double-skin facade using large-eddy simulation, Procedia Eng. 14 (2011) 3277–3284.
[38] O.A. Tkachenko, et al., Numerical and experimental investigation of unsteady natural convection in a non-uniformly heated vertical open-ended channel, Int. J. Therm. Sci. 99 (2016) 9–25.
[39] H. Wang, Z.(John, Zhai, Advances in building simulation and computational techniques: a review between 1987 and 2014, Energy Build. 128 (2016) 319–335.
[40] H. Choi, Y. An, K. Kang, S. Yoon, T. Kim, Cooling energy performance and thermal characteristics of a naturally ventilated slim double-skin window, Appl. Therm. Eng. 160 (2019) 114113.
[41] C. Popa, D. Ospir, S. Fohanno, C. Chereches, Numerical simulation of dynamical aspects of natural convection flow in a double-skin façade, Energy Build. 50 (2012) 229–233.
[42] T. Inan, T. Başaran, M.A. Ezan, Experimental and numerical investigation of natural convection in a double skin facade, Appl. Therm. Eng. 106 (2016) 1225–1235.
[43] T. Inan, T. Basaran, A. Erek, Experimental and numerical investigation of forced convection in a double skin façade, Energies 10 (9) (2017).
[44] A. Pappas, Z. Zhai, Numerical investigation on thermal performance and correlations of double skin façade with buoyancy-driven airflow, Energy Build. 40 (4) (2008) 466–475.
[45] G.K. Batchelor, Heat transfer by free convection across a closed cavity between vertical boundaries at different temperatures, Q. Appl. Math. 12 (3) (1954) 209–233.
[46] E.R.G. Eckertf, W.O. Carlson, Natural convection in an air layer enclosed between two vertical plates with different temperatures, Int. J. Heat Mass Tran. 2 (1–2) (1961) 106–110.
[47] L. Mei, et al., The influence of blinds on temperatures and air flows within ventilated double-skin facades, Proc. Clima (2007). WellBeing Indoors, 2007.
[48] O. Kalyanova, P. Heiselberg, Experimental Set-Up and Full-Scale Measurements in the 'Cube, Aalborg, 2008.
[49] W. Ding, Y. Hasemi, T. Yamada, Natural ventilation performance of a double-skin façade with a solar chimney, Energy Build. 37 (4) (2005) 411–418.
[50] F. Marques da Silva, M.G. Gomes, A.M. Rodrigues, Measuring and estimating airflow in naturally ventilated double skin facades, Build. Environ. 87 (2015) 292–301.
[51] E. Giancola, et al., Possibilities and challenges of different experimental techniques for airflow characterisation in the air cavities of façades, J. Facade Des. Eng. 6 (Aug. 2018), https://doi.org/10.7480/jfde.2018.3.2470. No 3 Spec. Issue FAÇADE 2018 – Adapt.
[52] K.J. King, Turbulent Natural Convection in Rectangular Air Cavities, Queen Mary University of London, 1989.
[53] N. Safer, "Modélisation des façades de type double-peau équipées de protections solaires : Approches multi-échelles, L'Institut National des Sciences Appliquées de Lyon, 2006.
[54] M. Bhamjee, A. Nurick, D.M. Madyira, An experimentally validated mathematical and CFD model of a supply air window: forced and natural flow, Energy Build. 57 (2013) 289–301.
[55] S.A. Kalogirou, in: E. Kalogirou (Ed.), Chapter 4 - Performance of Solar Collectors, Second, Academic Press, Boston, 2014, pp. 221–256. S. A. B. T.-S. E. E.
[56] Y. Hu, P.K. Heiselberg, H. Johra, R. Guo, Experimental and numerical study of a PCM solar air heat exchanger and its ventilation preheating effectiveness, Renew. Energy 145 (2020) 106–115.
[57] A. Janković, B. Lalić, Analysis of statistical methods for estimating solar radiation, Geogr. Pannonica 18 (1) (2014) 1–5.
[58] A. Hazem, M. Ameghchouche, C. Bougriou, A Numerical Analysis of the Air Ventilation Management and Assessment of the Behavior of Double Skin Facades, " *Energy Build.*, 2015.
[59] G. Michaux, R. Greffet, P. Salagnac, J.B. Ridoret, Modelling of an airflow window and numerical investigation of its thermal performances by comparison to conventional double and triple-glazed windows, Appl. Energy 242 (2019) 27–45.
[60] L.C.O. Souza, H.A. Souza, E.F. Rodrigues, Experimental and numerical analysis of a naturally ventilated double-skin façade, Energy Build. 165 (2018) 328–339.
[61] S. Preet, M.K. Sharma, J. Mathur, A. Chowdhury, S. Mathur, Performance evaluation of photovoltaic double-skin facade with forced ventilation in the composite climate, J. Build. Eng. 32 (2020) 101733.
[62] Y. Luo, L. Zhang, Z. Liu, L. Xie, X. Wang, J. Wu, Experimental study and performance evaluation of a PV-blind embedded double skin façade in winter season, Energy 165 (2018) 326–342.
[63] C. Lee, H. Lee, M. Choi, J. Yoon, Design optimization and experimental evaluation of photovoltaic double skin facade, Energy Build. 202 (2019) 109314.
[64] Y. Li, J. Darkwa, G. Kokogiannakis, Heat transfer analysis of an integrated double skin façade and phase change material blind system, Build. Environ. 125 (2017) 111–121.
[65] Y. Li, J. Darkwa, G. Kokogiannakis, W. Su, Phase change material blind system for double skin façade integration: system development and thermal performance evaluation, Appl. Energy 252 (2019) 113376.
[66] J. Curpek, M. Cekon, J. Hraska, PCM integrated in BiPV ventilated Facąde concepts: experimental test cell platform and initial full-scale measurements, IOP Conf. Ser. Earth Environ. Sci. 290 (1) (2019) 12072.
[67] H. Elarga, F. Goia, A. Zarrella, A. Dal Monte, E. Benini, Thermal and electrical performance of an integrated PV-PCM system in double skin façades: a numerical study, Sol. Energy 136 (2016) 112–124.
[68] K. Cho, D. Cho, Solar heat gain coefficient analysis of a slim-type double skin window system: using an experimental and a simulation method, Energies 11 (1) (Jan. 2018) 115.
[69] C. Zhang, W. Gang, J. Wang, X. Xu, Q. Du, Numerical and experimental study on the thermal performance improvement of a triple glazed window by utilizing low-grade exhaust air, Energy 167 (2019) 1132–1143.
[70] F. Yang, F. Yuan, F. Qian, Z. Zhuang, J. Yao, Summertime thermal and energy performance of a double-skin green facade: a case study in Shanghai, Sustain. Cities Soc. 39 (2018) 43–51.
[71] X. Hong, M.K.H. Leung, W. He, Effective use of Venetian blind in Trombe wall for solar space conditioning control, Appl. Energy 250 (Sep. 2019) 452–460.
[72] O. Iken, S. ed-D. Fertahi, M. Dlimi, R. Agounoun, I. Kadiri, K. Sbai, Thermal and energy performance investigation of a smart double skin facade integrating vanadium dioxide through CFD simulations, Energy Convers. Manag. 195 (2019) 650–671.
[73] Z. Liang, et al., Tungsten-doped vanadium dioxide thin films as smart windows with self-cleaning and energy-saving functions, J. Alloys Compd. 694 (2017) 124–131.
[74] G. Baldinelli, Double skin façades for warm climate regions: analysis of a solution with an integrated movable shading system, Build. Environ. 44 (6) (2009) 1107–1118.
[75] A. Zöllner, E.R.F. Winter, R. Viskanta, Experimental studies of combined heat transfer in turbulent mixed convection fluid flows in double-skin-façades, Int. J. Heat Mass Tran. 45 (22) (2002) 4401–4408.
[76] H. Manz, A. Schaelin, H. Simmler, Airflow patterns and thermal behavior of mechanically ventilated glass double facades, Build. Environ. 39 (9) (2004) 1023–1033.
[77] I. Pérez-Grande, J. Meseguer, G. Alonso, Influence of glass properties on the performance of double-glazed facades, Appl. Therm. Eng. 25 (17–18) (Dec. 2005) 3163–3175.
[78] T.E. Jiru, Y.X. Taob, F. Haghighat, Airflow and heat transfer in double skin facades, Energy Build. 43 (10) (2011) 2760–2766.
[79] F. Kuznik, T. Catalina, L. Gauzere, M. Woloszyn, J.J. Roux, Numerical modelling of combined heat transfers in a double skin faade - full-scale laboratory experiment validation, Appl. Therm. Eng. 31 (14–15) (2011) 3043–3054.
[80] A. Guardo, M. Coussirat, E. Egusquiza, P. Alavedra, R. Castilla, A CFD approach to evaluate the influence of construction and operation parameters on the performance of Active Transparent Façades in Mediterranean climates, Energy Build. 41 (5) (2009) 534–542.
[81] S. Yan, X. Li, B. Wang, W. Shi, W. Lyu, A method to describe the thermal property of pipe-embedded double-skin façade: equivalent glass window, Energy Build. 195 (2019) 33–44.
[82] J. Curpek, M. Cekon, J. Hraska, PCM integrated in BiPV ventilated façade concepts: experimental test cell platform and initial full-scale measurements, IOP Conf. Ser. Earth Environ. Sci. 290 (2019), 012072.
[83] S.P. Corgnati, M. Perino, V. Serra, Experimental assessment of the performance of an active transparent façade during actual operating conditions, Sol. Energy 81 (8) (Aug. 2007) 993–1013.
[84] D. Saelens, Energy Performance Assessment of Single Storey Multiple-Skin Facades, Catholic University of Leuven, 2011.
[85] E. Colombo, M. Zwahlen, M. Frey, J. Loux, Design of a glazed double-façade by means of coupled CFD and building performance simulation, Energy Procedia 122 (2017) 355–360.
[86] Y. Katoh, M. Miyamoto, J. Kurima, S. Kaneyasu, "Turbulent free convection heat transfer from vertical parallel Plates : effect of entrance bell-mouth shape, in: JSME Int. journal. Ser. 2, Fluids Eng. heat Transf. power, Combust. Thermophys. Prop. 34, 1991, pp. 496–501, 4.
[87] Y. Cherif, E. Sassine, S. Lassue, L. Zalewski, Experimental and numerical natural convection in an asymmetrically heated double vertical facade, Int. J. Therm. Sci. 152 (2020) 106288.
[88] A.A. Dafa'Alla, P.L. Betts, Experimental study of turbulent natural convection in a tall air cavity, Exp. Heat Tran. 9 (2) (1996) 165–194.
[89] D. Saelens, J. Carmeliet, H. Hens, Energy performance assessment of multiple-skin facades, HVAC R Res. 9 (2) (2003) 167–185.
[90] A. Dama, D. Angeli, O. Kalyanova Larsen, Naturally ventilated double-skin façade in modeling and experiments, Energy Build. 114 (2017) 17–29.
[91] S. Hassanli, K.C.S. Kwok, M. Zhao, Performance assessment of a special Double Skin Façade system for wind energy harvesting and a case study, J. Wind Eng. Ind. Aerod. 175 (2018) 292–304.
[92] T. Zhang, H. Yang, Flow and heat transfer characteristics of natural convection in vertical air channels of double-skin solar façades, Appl. Energy 242 (2019) 107–120.
[93] K. Hou, S. Li, H. Wang, Simulation and experimental verification of energy saving effect of passive preheating natural ventilation double skin façade, Energy Explor. Exploit. (Sep. 2020), 0144598720956288.
[94] S. El Ahmar, F. Battista, A. Fioravanti, Simulation of the thermal performance of a geometrically complex Double-Skin Facade for hot climates: EnergyPlus vs OpenFOAM, Build. Simul. 12 (5) (2019) 781–795.
[95] N. Kimouche, Z. Mahri, A. Abidi-Saad, C. Popa, G. Polidori, C. Maalouf, Effect of inclination angle of the adiabatic wall in asymmetrically heated channel on natural convection: application to double-skin façade design, J. Build. Eng. 12 (2017) 171–177.

[96] E. Sanchez, A. Rolando, R. Sant, L. Ayuso, Influence of natural ventilation due to buoyancy and heat transfer in the energy efficiency of a double skin facade building, Energy Sustain. Dev. 33 (2016) 139–148.
[97] B. Koo, K. Lee, Y. An, K. Lee, Solar heat gain reduction of ventilated double skin windows without a shading device, Sustainability 10 (2) (Dec. 2017) 64.
[98] I.A.E.-K.M. Amaireh, Numerical Investigation into a Double Skin Façade System Integrated with Shading Devices, with Reference to the City of Amman, University of Nottingham, Jordan, 2017.
[99] D.D. Kim, Computational fluid dynamics assessment for the thermal performance of double-skin façades in office buildings under hot climatic condition, Build. Serv. Eng. Technol. (Aug. 2020), 0143624420952962.
[100] Y. Tao, H. Zhang, L. Zhang, G. Zhang, J. Tu, L. Shi, Ventilation performance of a naturally ventilated double-skin façade in buildings, " *Renew. Energy*, 2020.
[101] E. Lee, S. Selkowitz, V. Bazjanac, V. Inkarojrit, C. Kohler, High-Performance Commercial Building Façades, Berkeley, 2002.
[102] D. Angeli, A. Dama, Modelling natural ventilation in double skin facade, Energy Procedia 78 (2015) 1537–1542.
[103] S. Hassanli, K. Chauhan, M. Zhao, K.C.S. Kwok, Application of through-building openings for wind energy harvesting in built environment, J. Wind Eng. Ind. Aerod. 184 (2019) 445–455.
[104] S. Hassanli, G. Hu, D.F. Fletcher, K.C.S. Kwok, Potential application of double skin façade incorporating aerodynamic modifications for wind energy harvesting, J. Wind Eng. Ind. Aerod. 174 (2018) 269–280.
[105] S. Matour, V. Garcia Hansen, R. Drogemuller, S. Omrani, S. Hassanali, Natural ventilation of double skin façade: evaluation of wind-induced airflow in tall buildings, in: 35th PLEA Conference Sustainable Architecture and Urban Design Planning: Post Carbon Cities, 2020.
[106] S. Hassanli, G. Hu, K.C.S. Kwok, D.F. Fletcher, Utilizing cavity flow within double skin façade for wind energy harvesting in buildings, J. Wind Eng. Ind. Aerod. 167 (2017) 114–127.
[107] B. Bielek, D. Szabó, M. Palko, M. Rychtáriková, Optimisation of design of air inlets in air distribution channels of a double-skin transparent façade, Slovak J. Civ. Eng. 25 (4) (2017) 1–11.
[108] M.N. Sánchez, E. Giancola, E. Blanco, S. Soutullo, M.J. Suárez, Experimental validation of a numerical model of a ventilated façade with horizontal and vertical open joints, Energies 13 (1) (Dec. 2019) 146.
[109] N. Pourshab, M.D. Tehrani, D. Toghraie, S. Rostami, Application of double glazed façades with horizontal and vertical louvers to increase natural air flow in office buildings, Energy 200 (2020) 117486.
[110] H. El-Sadi, F. Haghighat, A. Fallahi, CFD analysis of turbulent natural ventilation in double-skin fąade: thermal mass and energy efficiency, J. Energy Eng. 136 (3) (2010) 68–75.
[111] Y. Ji, M.J. Cook, V. Hanby, D.G. Infield, D.L. Loveday, L. Mei, CFD modelling of naturally ventilated double-skin facades with Venetian blinds, J. Build. Perform. Simul. 1 (3) (2008) 185–196.
[112] V.I. Hanby, et al., Nodal network and CFD simulation of airflow and heat transfer in double skin facades with blinds 29 (1) (2008) 45–59.
[113] D. Iyi, R. Hasan, R. Penlington, C. Underwood, Double skin fa??ade: modelling technique and influence of Venetian blinds on the airflow and heat transfer, Appl. Therm. Eng. 71 (1) (2014) 219–229.
[114] C. Jiménez-Xamán, et al., Solar chimneys with a phase change material for buildings: an overview using CFD and global energy balance, Energy Build. 186 (2019) 384–404.
[115] J.P. Varughese, M.M. John, Effect of emissivity of shading device and air flow inside cavity of Double Skin Facade for energy saving and Thermal Comfort in buildings: a CFD modeling, in: 2016 International Conference on Energy Efficient Technologies for Sustainability, ICEETS 2016, 2016, pp. 815–820.
[116] Y. Li, J. Darkwa, W. Su, Investigation on thermal performance of an integrated phase change material blind system for double skin façade buildings, Energy Procedia 158 (2019) 5116–5123.
[117] Y. Li, J. Darkwa, G. Kokogiannakis, W. Su, Effect of design parameters on thermal performance of integrated phase change material blind system for double skin façade buildings, Int. J. Low Carbon Technol. 14 (2) (Jun. 2019) 286–293.
[118] C. Shen, X. Li, Solar heat gain reduction of double glazing window with cooling pipes embedded in Venetian blinds by utilizing natural cooling, Energy Build. 112 (2016) 173–183.
[119] C. Shen, X. Li, Thermal performance of double skin façade with built-in pipes utilizing evaporative cooling water in cooling season, Sol. Energy 137 (2016) 55–65.
[120] M. Coussirat, A. Guardo, E. Jou, E. Egusquiza, E. Cuerva, P. Alavedra, Performance and influence of numerical sub-models on the CFD simulation of free and forced convection in double-glazed ventilated façades, Energy Build. 40 (10) (2008) 1781–1789.
[121] R. Fuliotto, F. Cambuli, N. Mandas, N. Bacchin, G. Manara, Q. Chen, Experimental and numerical analysis of heat transfer and airflow on an interactive building facade, Energy Build. 42 (1) (Jan. 2010) 23–28.
[122] Z. Zeng, X. Li, C. Li, Y. Zhu, Modeling ventilation in naturally ventilated double-skin façade with a Venetian blind, Build. Environ. 57 (2012) 1–6.
[123] D. Brandl, T. Mach, M. Grobbauer, C. Hochenauer, Analysis of ventilation effects and the thermal behaviour of multifunctional façade elements with 3D CFD models, Energy Build. 85 (2014) 305–320.
[124] X. Hong, W. He, Z. Hu, C. Wang, J. Ji, Three-dimensional simulation on the thermal performance of a novel Trombe wall with Venetian blind structure, Energy Build. 89 (2015) 32–38.
[125] T. Başaran, T. İnan, Experimental investigation of the pressure loss through a double skin facade by using perforated plates, Energy Build. 133 (2016) 628–639.
[126] T. Inan, T. Basaran, Experimental and numerical investigation of forced convection in a double skin façade by using nodal network approach for Istanbul, Sol. Energy 183 (2019) 441–452.
[127] W. Chiu, F.J. Rixon, High resolution structural studies of complex icosahedral viruses: a brief overview, Virus Res. 82 (1–2) (2001) 9–17.
[128] R. Li, A. Pitts, Y. Li, Buoyancy-driven natural ventilation of a room with large openings, in: IBPSA 2007 - International Building Performance Simulation Association 2007, 2007, pp. 984–991.
[129] G. He, L. Shu, S. Zhang, Double skin facades in the hot summer and cold winter zone in China: cavity open or closed? Build. Simul. 4 (4) (2011) 283–291.
[130] S. Tkachenko, V. Timchenko, Yeoh, Heng Guan, J.A. Reizes, Effects of radiation on turbulent natural convection in channel flows, Int. J. Heat Fluid Flow 77 (2019) 122–133.
[131] V. Sambou, "Transferts thermiques instationnaires: vers une optimisation de parois de bâtiments." Université de Toulouse, Université Toulouse III-Paul Sabatier, 2008.
[132] T. Yilmaz, S.M. Fraser, Turbulent natural convection in a vertical parallel-plate channel with asymmetric heating, Int. J. Heat Mass Tran. 50 (13–14) (2007) 2612–2623.
[133] B.W. Webb, D.P. Hill, High Rayleigh number laminar natural convection in an asymmetrically heated vertical channel, J. Heat Tran. 111 (3) (1989) 649–656.